Deposition of Colloidal Quantum Dots by Microcontact Printing for LED Display Technology

by

LeeAnn Kim

Submitted to the Department of Electrical Engineering and Computer Science
in partial fulfillment of the requirements for the degree of

Masters of Engineering in Electrical Engineering and Computer Science

at the

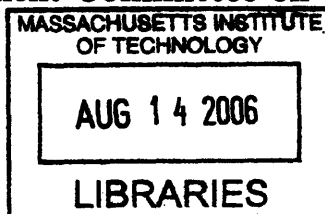MASSACHUSETTS INSTITUTE OF TECHNOLOGY

February 2006

Author . . . .
Department of Electrical Engineering and Computer Science
January 2006

Certified by . . . .
Vladimir Bulović
Associate Professor, KDD Career Development Chair
Thesis Supervisor

Accepted by . . . .
Arthur C. Smith
Chairman, Department Committee on Graduate Students

Deposition of Colloidal Quantum Dots by Microcontact Printing for LED Display Technology

by

LeeAnn Kim

Submitted to the Department of Electrical Engineering and Computer Science
on January 2006, in partial fulfillment of the
requirements for the degree of
Master of Engineering in Electrical Engineering and Computer Science

Abstract

This thesis demonstrates a new deposition method of colloidal quantum dots within a quantum dot organic light-emitting diode (QD-LED). A monolayer of quantum dots is microcontact printed as small as 20 μm lines as well as millimeter scale planes, and the resulting devices show quantum efficiencies as high as 1.2% and color saturation superior to previous QD-LEDs'. Through a modification of the polydimethylsiloxane (PDMS) stamp with a parylene-C coating, quantum dots solvated in chloroform were successfully inked and stamped onto various substrates, including different molecular organic layers. The ability to control the placement and the pattern of the quantum dots independently from underlying organic layers provides a new level of performance in QD-LEDs, increasing the possibility of QD-LED displays.

Thesis Supervisor: Vladimir Bulović
Title: Associate Professor, KDD Career Development Chair

Acknowledgments

Contents

List of Figures

Chapter 1

Introduction

An organic light-emitting diode, also known as an OLED, is an emerging display technology. As information continues to become densified, manipulated, and traded at rates faster than ever, the visual medium has become critical and technologically sophisticated. From televisions to computers, music players and cameras, it is difficult to avoid displays. There always seems to be a demand for displays that trump the current best. More color, more light, better detail. Recently, OLEDs that incorporated a new type of material, called quantum dots (QDs), demonstrated the potential to improve OLED display performance.

OLEDs consist of organic layers that transport electrons from the cathode and holes from the anode, to create excited state electron-hole pairs called excitons. These excitons relax on a molecular site and emit light. When quantum dots are included in the organic layers, some of the exciton relaxation occur on the dots, resulting in light characteristic of the quantum dot. Emission from quantum dots is notable, in particular because its color-tunability and color purity far exceed that of organic molecules. A recent demonstration of a new QD-LED device architecture showed the possibility of having most of the light emission occur from the quantum dots, as opposed to from the organics. The placement of a monolayer of quantum dots, at the correct interface between two organic layers, results in an efficient and superior color device. However, the method employed to generate such a monolayer does not allow for the patterning of pixels required for displays. It also introduces impurities

through solvent exposure.

This thesis continues the work of QD-LEDs by developing a device-compatible quantum dot deposition technology. It explores the possibility of microcontact printing as a way to pattern the quantum dot monolayer film and protect the underlying organic layer from degradation. A brief discussion is presented on other patterning techniques that are used in both the traditional printing field and within the organic field. The issue of obtaining a well-formed monolayer film by microcontact printing is then addressed and, through use of surface control, the desired film is achieved and patterned into devices.

Chapter 2

Displays

The purpose of an electronic display is to communicate information to people through images. Its design is therefore determined by how a viewer receives and interprets optical signals. We begin with a discussion on how colors are perceived, and the spatial and temporal acuity of the human visual system.

We then discuss two of the most dominant display technologies that are currently in use, the cathode ray tube (CRT) and the liquid crystal display (LCD).

2.1 Human Visual Perception

2.1.1 Color

The visible part of the electromagnetic wave spectrum covers from 770 nm to 380 nm, red to blue. It is a very narrow slice of the EM specrum, to which human eye receptors have a special sensitivity. The eye is made up of two types of light receptor cells – cones and rodes – which lie on the retina, the innermost layer of the eyeball. The rods are luminosity sensors, and relay only grayscale information about luminance levels. Cones can differentiate between different wavelengths of light, for the perception of color. There are three different subtypes of cones: short-wavelength cells peak around 440 nm, medium at 540 nm, and long at 565 nm. These cones work together to interpret a spectral distribution in form of a perceived color [2].
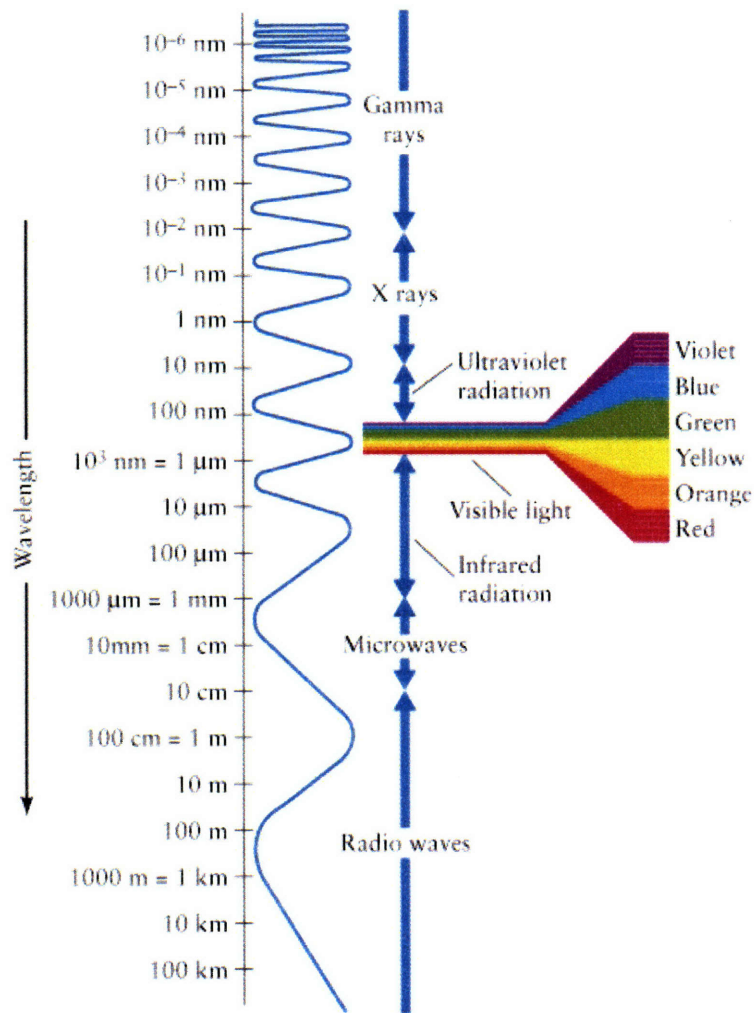
Figure 2-1: Electromagnetic spectrum. [1]
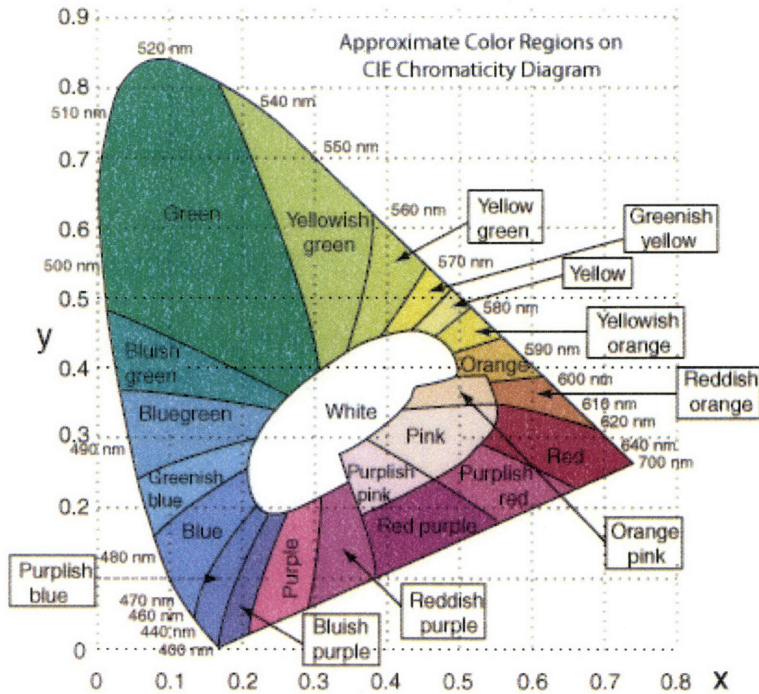
Figure 2-2: CIE diagram which maps any XY coordinate calculated from a spectral distribution onto a distinct perceived color. Approximation of the color regions are shown and not a representation of the true color.

Different spectral distributions can be perceived as exactly the same color. For instance, the combination of a red and green light will produce the sensation "yellow", as would a spectrally pure monochrome light with a wavelength of 600 nm. In 1931, the Committee International de l'Eclairage developed a useful model for the spectral sensitivity of the cones (Fig. 2-3). By using these curves and the spectral distribution of light entering the eyes, a set of three values are obtained that uniquely define the color interpreted by the eye-brain system. The CIE chromaticity diagram charts these coordinates (Fig. 2-2).

The edge of the CIE diagram represents pure colors. These edges can only be attained by single wavelength electromagnetic radiation, and their combination can give any color within the horseshoe shaped boundary of the chart they define. If three points are chosen on the CIE diagram, the colors within the triangle defined will be producible by a weighted mixture of those three colors corresponding to the corners. The conclusion is then that the more saturated the colors of the corners are,
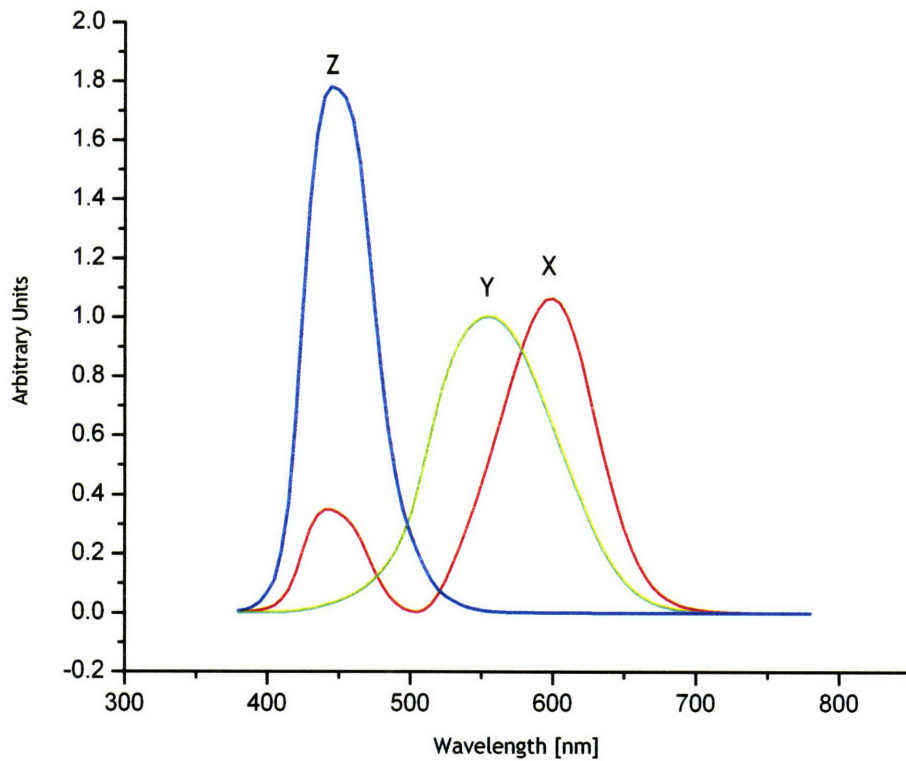
Figure 2-3: Multiplying each sensitivity curve above with the spectral distribution of the light source, integrating the results and normalizing all three values to add to 1, will give the X, Y and Z values corresponding to CIE coordinates. It should be noted that these curves are not the same as the actual sensitivity curves of the cones. They have been modified for practical modelling reasons.
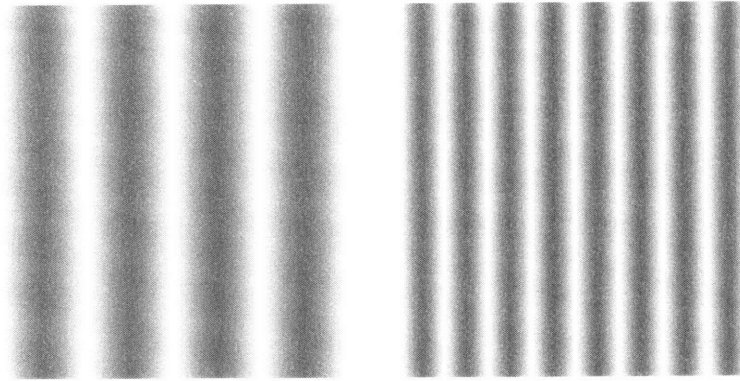
Figure 2-4: Sinusoidal pattern used to determine the spatial limit of the human eye. [2]

the wider the range of attainable colors. A saturated light source is characterized by a very narrow linewidth emission spectrum.

2.1.2 Spatial Response: Resolution

The ability to discern details is called visual acuity, and it is often measured by determining the smallest distance in which change of luminance or color is detectable by the human eye. It is undersirable for a viewer to be able to discern pixilation of an image on a display screen. The illusion of spatial continuity that mimics how people see the actual world is important to users of electronic displays, for practical and emotional reasons. If given a sinusoidal pattern of alternating dark and light lines (Fig. 2-4, the human eye will be at the limit of visual acuity at the frequency those lines indistinguishably merge. Visual acuity peaks at approximately 10-30 cycles per visual degree, and is generally assumed to reach a limit around 50-60 cycles per visual degree. This upper limit translates to roughly 300-600 dots per inch, or around 85μm $- 42\mu$m large pixels (where a pixel is three subpixels of red, green, and blue). To make a display with a resolution that exceeds this specification would provide no gain because of the physiological limit of the eye.

21

2.1.3 Temporal Response: Refresh Rate

Human eyes take in information at a finite rate. Even though it seems like we view the world in a continuous fashion, in actuality the eye takes in discrete "snapshots" which the brain processes into one continuous motion. This is because it takes time for receptors to respond, signals to be sent to the brain, and the receptors to reset in preparation for the next set of signals. This property of the human visual system allows quick succession of frames to be seen as one fluid motion, and an electronic display only needs to show a succession of still frames at a fast enough rate to emulate smooth motion. However, the rate varies because the eye is sensitive to change in illumination intensities, so movies played in a dark theatre are played at 24 frames/s, while televisions refresh at a rate of 50 or 60 images per second. If this rate is too slow, not only does the motion look unrealistic, but the luminance also appears inconstant resulting in a "flicker" effect. To avoid this flicker, a display needs to refresh in the range of 60-85 cycles per second.

2.2 Present Technology

2.2.1 CRT

The cathode ray tube technology is more than 100 years old. It is the cheapest display form and still maintains a prevalent position. One of the last widely used application of the vacuum tube, the CRT works by shooting an energetic beam of electrons at a screen of different colored phosphors. This beam can be bent and directed at different parts of the screen, illuminating any one point of the complete image. The standard scheme to produce a whole image is to have the beam scan each horizontal line, starting from the top and moving to the bottom. Done quickly enough, the viewer sees one complete frame, and if the frames are updated quickly enough, one fluid motion.

The advantages of the CRT are that it is a mature and cost competitive technology. In almost all areas, including color, viewing angles, resolution, brightness, and speed,
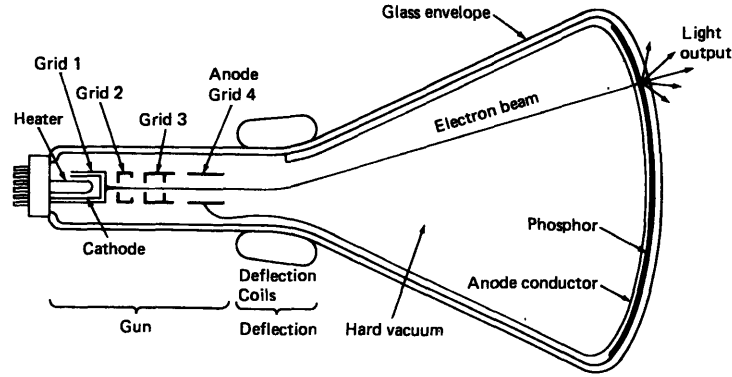
Figure 2-5: Schematic of a cathode-ray tube, the bulky standard television display. [3]

the CRT performs very solidly. However, its size has been a primary drawback that has motivated the unrelenting development and refinement of flat-panel displays. Because of the vacuum tube, a CRT display is bulky in terms of depth, and also heavy. It is not readily portable nor easily insertable into many applications that require a display.

2.2.2 LCD

The liquid crystal display (LCD) uses the property that liquid crystals can exist in different phases, some more ordered than others depending on temperature, and can be made to align through a field effect. By applying a voltage across the liquid crystal, the light that reaches the viewer can be modulated between off and on, sometimes with the additional use of a polarizing sheet. One scheme is shown in Fig. 2-6. For color LCDs, the light that passes through the liquid crystals is then passed through red, green, and blue filters.

LCDs are the dominant flat-panel display at the moment. They appear in many different applications, most familiarly in laptops and digital camera viewfinders. However, they show weaknesses in several areas that have prevented penetration into large surface area and video applicaitons. Viewing angles are narrow compared to other display technologies. Color range is underwhelming, and power efficiency is lowered because of the use of filters. Switching speeds between off and on states are in the
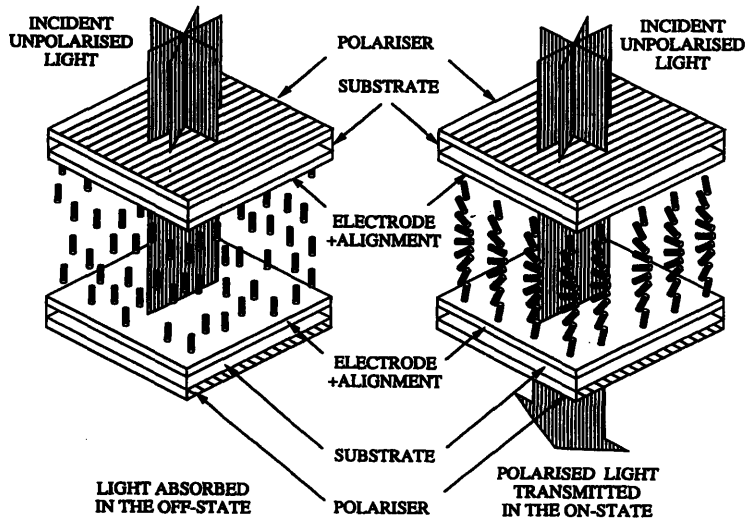
Figure 2-6: Schematic of the liquid crystal display. [4]

milliseconds due to LC effects as well as the crystals themselves requiring time to respond. For high-quality video, LCD's slow response time produces artifacts such as blurring and choppiness. Finally because of the layered complexity, manufacturing of LCDs is hard to make cost effective.

Chapter 3

QD-LED Background

Alternatives to CRTs and LCDs, the two dominant display technologies, exist. An example is the plasma display, which is an expensive, high definition, thin-form alternative to the CRT television screen. Another example, the subject of this work, is the organic light-emitting diode (OLED). In this section, we discuss the more traditional inorganic light emitting diode (LED), the newer organic LED, and then a variation upon the organic form that uses quantum dots.

3.1 LED

The inorganic light-emitting diode, simply referred to as an LED, emits light by passing current through an emissive layer. Recently, LEDs have been showing up in direct-viewing applications such as traffic lights and indicator lights, but not as much in full-color displays for television and monitors. One of the main reasons for this is the cost of fabricating LEDs. The most simplistic version is a dual single-crystal semiconductor epitaxially grown to form a p-n junction. High quality epitaxial growth is an expensive, slow process. However, it is an inherently thin form device. In addition, LEDs have superior viewing angles and better power usage because of the lack of filters that absorb some of the light emissions. Yet, due to fabrication requirements, superior LED efficiencies, colors, and viewing angles are not enough to compete with the popularity of LCDs.

3.2 OLED

Organic light-emitting diodes could address this missing element of easy, cheap manu-facturability while maintaing the potential for superior color and brightness, contrast, power efficiency, as well as fast time responses, wide viewing angles, and simplified manufaturability [8]. Organic semiconductors were recognized as potential electro-luminescent lumophores over fifty years ago. But problems such as instability and low-carrier mobilities made organic light-emitters elusive [9]. The earliest reports of electroluminescence (EL) from organic materials used very thick films of anthracene and had operating voltages in the hundreds of volts [10][11]. It took another twenty years until Ching Tang demonstrated a reasonable device that operated at less than 10V through the use of a new device structure [12][13]. With the demonstration of polymer organic devices by Burroughes et al. [14] a few years later, the work touched off the field of organic LEDs.
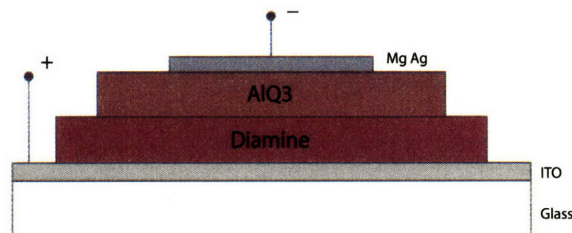
Figure 3-1: A heterojunction organic device, which contains two organic layers, of which at least one exclusively transports a single type of charge. This effectively determines where excitons are formed.

Tang's OLED consisted of a heterojunction of two relatively thin organic layers, one capable of transporting only one type of charge. Present day OLEDs, which still make use of this multi-junction architecture, continue to make improvements in quantum efficiencies, color, and lifetime. While they are viewed as a serious alter-native to other light technologies, to date they have appeared mostly in smal-scale,

short lifetime applications, such as camera displays and cellphone indicators and displays. They have yet to achieve performance numbers that are convincing of their competitiveness in the large-display industry.
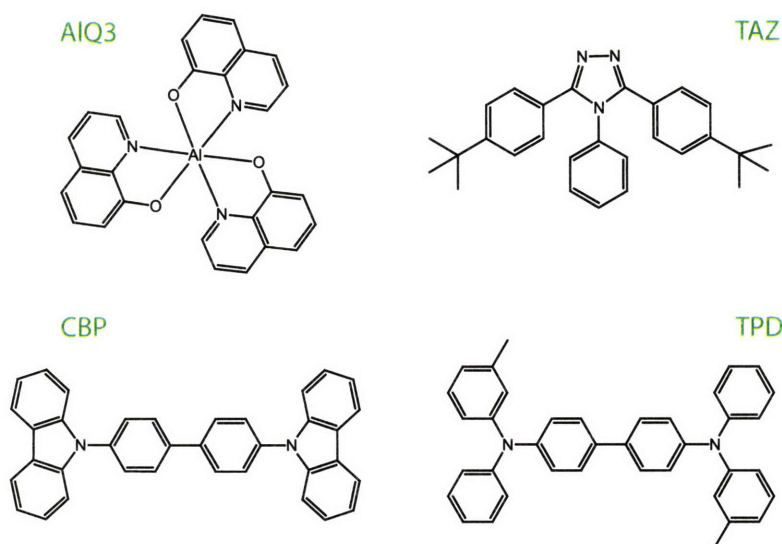
Figure 3-2: Typical small-molecule organics. Tris-(8-hydroxyquinoline) aluminum known as Alq_3. 3,5-Bis(4-tert-butyl-phenyl)-4-phenyl-[1,2,4]triazole known as TAZ. 4,4'-Bis(carbazol-9-yl)biphenyl known as CBP. N,N'-Bis(3-methylphenyl)-N,N'-bis-(phenyl)-benzidine known as TPD. CBP and TPD are hole transporters and AlQ_3 is an electron transporter, while TAZ acts as a hole blocker. The AlQ_3 is often also the luminescent layer.

3.3 QD-LED

3.3.1 Quantum Dots

Quantum dots are nanoscale semiconductor spheres that exhibit properties deviating from that of the bulk due to quantum confinement. As a nanocrystal shrinks in size and becomes smaller than the bulk exciton diameter, the HOMO and LUMO gap widens and the emission is blue-shifted. Precise control over the wavelength of emission is given by a straightforward selection of crystallite size [15], while using the same basic synthetic procedure. Because of the discretization of the density of

states at the band edge, emission becomes narrowed due to quantum confinement. A typical photoluminescence FWHM is 30nm or less. This spectral narrowing is important because it is an indication of the color purity of emitted light. As shown before with the CIE diagram, the more saturated the set of base mixing colors, the more extensive the full palette is.
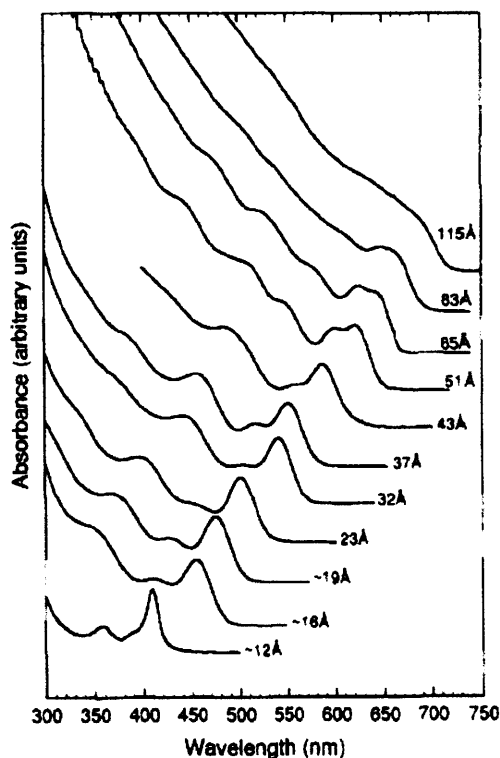
Figure 3-3: Absorption spetra of CdSe QDs, size tuned from 12 to 115 Å. [5]

The quantum dots that are used in this work are colloidally grown core/shell quantum dots with a passivating organic capping group. At the surface of the quantum dot, the crystallinity of the semiconductor is interrupted because of the lack of the appropriate number of neighboring molecules. The surface states act as traps that provide for nonradiative recombination, which lowers the efficiency of the dots. By epitaxially growing a shell layer of a wider bandgap semiconductor material, the quantum dot surface can be passivated [16]. A prime example is a CdS coated CdSe quantum dot [17]. The final layer of organic capping allows the quantum dots to be solvated in organic solvents, and therefore processable much in the same manner as

organic molecules. The organic cappings also prevent aggregation and precipitation of the quantum dots. Some common organic cappings include oleic acid, pyridine, trioctylphosphine oxide, and thiols.
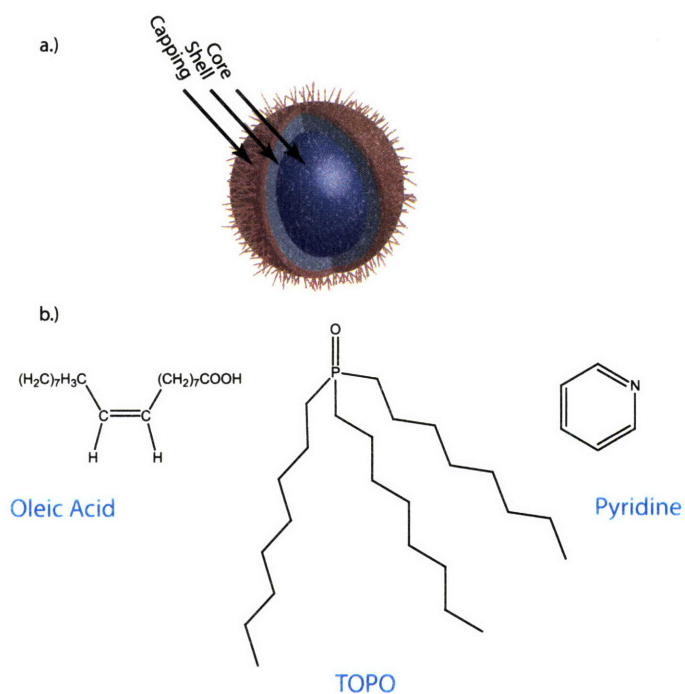
Figure 3-4: a) Structure of core-shell quantum dot, with organic capping. b) Various cappings for quantum dots, such as oleic acid, trioctylphosphine oxide, and pyridine. The most common capping on the quantum dots for this work are TOPO.

Using CdSe QD as an example, the colors that can be attained by tuning range from 1.7 eV which corresponds to the bulk, and a wavelength in the far red of 730 nm, to 2.75 eV which corresponds to a blue wavelength of 450 nm [5]. Capable of accessing this wide range of colors, exhibiting narrow linewidths, and being made up of inorganic materials that are potentially more stable against oxidation compared to organic molecules, the quantum dot may be the ideal, alternative lumophore to enhance OLED performance.

3.3.2 Hybrid Inorganic/Organic Device

OLEDs that contain quantum dots as the lumophore are referred to as QD-LEDs. In 1994, Vicki Colvin et al. fabricated a hybrid polymer/QD-LED displaying prominent

QD electroluminescence characteristics with external efficiences between 0.001% and 0.01% [18]. In 2002, Seth Coe et al. demonstrated a QD-LED with a peak quantum efficiency of 0.52% [19], and have continued to improve the efficiencies. Those devices incorporate only a monolayer of quantum dots as the luminescent layer inbetween organic layers. They show high brightness and small spectral FWHM, and the technique for making such devices was shown to be applicable to a wide range of particle materials, dimensions, and shapes [20]. These improvements were attained by a device architecture in which the quantum dots were physically isolated to a well-ordered monolayer between the organic layers.
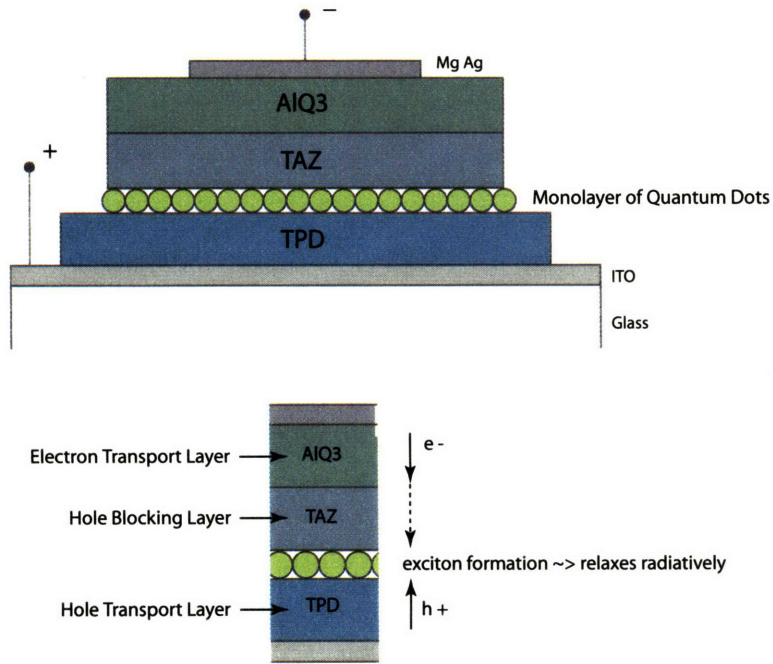
Figure 3-5: An OLED with a single monolayer of well-ordered quantum dots placed at the interface between the hole transporting layer and the hole blocking layer.

The monolayer sandwich structure drastically improves the QD-LED quantum efficiency because charge transport isn't hindered by highly resistive quantum dots. The organic semiconductors act as the hole and electron transport layers, electron-hole pairs called excitons form near or on the quantum dot, and then those excitons

relax within the dots resulting in radiative emission. In this manner, the ratio of quantum dot emission to organic emission is dramatically increased allowing for the device light output to be almost solely defined by the quantum dot.

3.3.3 Deposition of Monolayer QD Film

Small molecule organic film deposition is most commonly done by thermal evaporation techniques in high vacuum environments. In contrast, depositions of polymeric molecules use methods such as dip-coating or spin-casting out of solution. Both types of organics and respective deposition methods present advantages and disadvantages, but for quantum dots, thermal evaporation is not an option because of their size, weight, and composition. Before the monolayer device, QD-LED devices were made by spin-casting a thick layer of quantum dots on top of a polymer layer such as PPV [18][21].
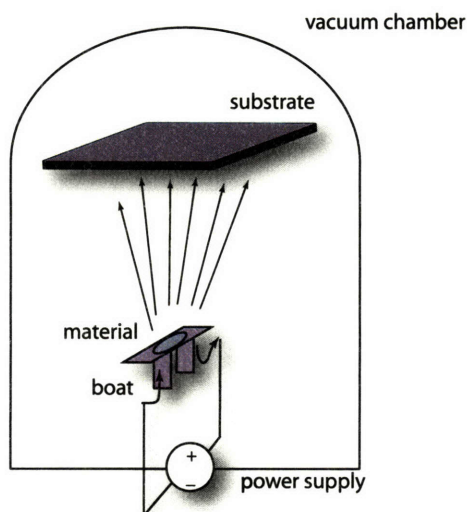
Figure 3-6: Thermal evaporation chamber, in which current runs through a boat holding the desired material to be deposited. As the resistive boat heats up, the material sublimes and condenses when it hits the substrate above.

The monolayer films are formed by spin-casting quantum dots, while also utilizing the principle of phase separation. A chloroform solution of small molecule organic and quantum dots are spin-cast at appropriate concentration and spin parameters,

resulting in the quantum dots rising above the layer of small molecule organics in a neat hexagonally close packed film.

1. solution of quantum dots/TPD/chloroform

2. dropped onto a substrate, which is then spun

3. spinning dries the solution as well as spreads it out and phase separates the quantum dots from TPD

4. leaving behind a thin film of TPD layered below a thin film of quantum dot

spin

TPD
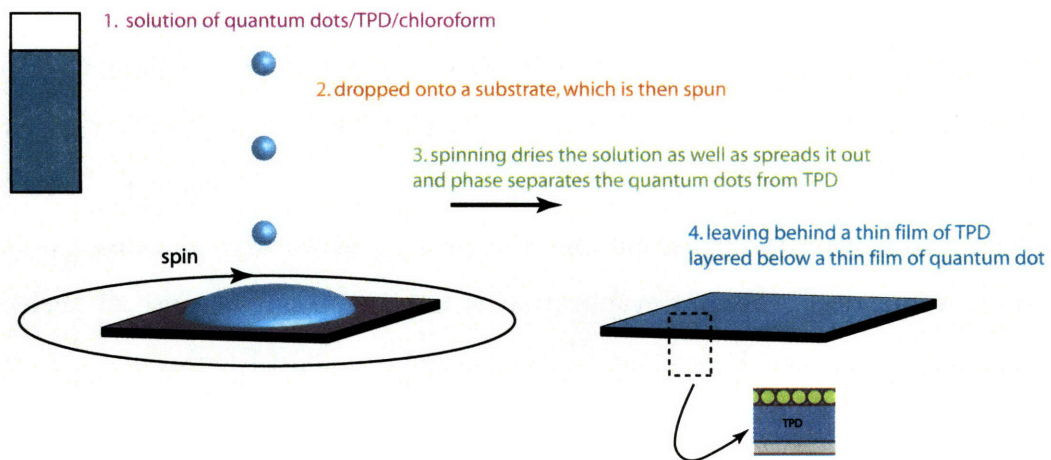
Figure 3-7: Spincasting procedure and phase separation principles form the well-ordered quantum dot film atop TPD.
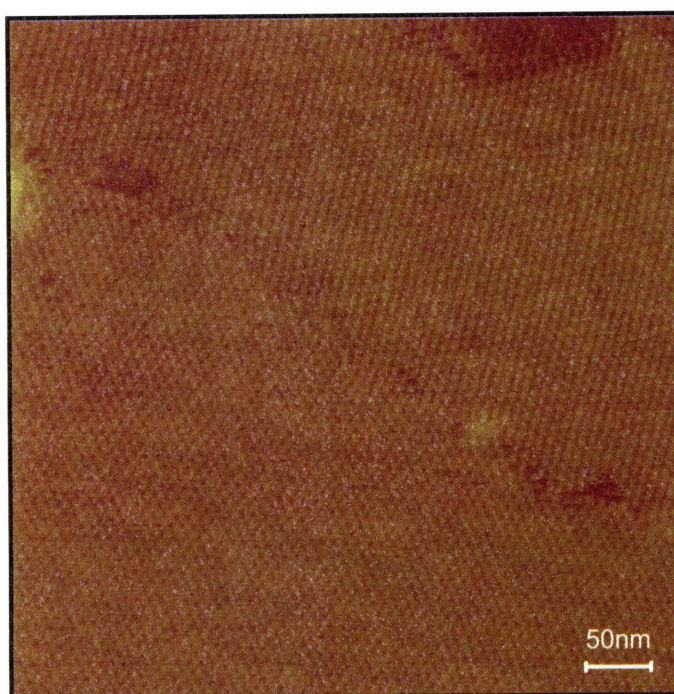
Figure 3-8: AFM of monolayer of well-packed quantum dot atop organic molecule TPD.

Chapter 4

Printing and Patterning Background

A QD-LED display requires devices that are small enough to meet the requirements of the human visual system, and these devices must be placed next to each other in a precise and regular layout. Just like the optical lithographic methods in the microelectronics industry that produces chips of tiny components with high throughput and precision, these displays need a patterning technique. Ultimately, this work will focus on a microcontact printing method to achieve patterning capability.

This section gives background on traditional printing and patterning methods. We then review the concepts of microcontact printing and microtransfer molding, since these two patterning techniques are further discussed in the experimental chapter.

4.1 Traditional Methods

The invention of printing is an important milestone in the history of civilization. It is a communication technology that mass reproduces and distributes ideas over distance and time. Printing techniques have traditionally fallen into four main categories: relief, intaglio, lithography, and silkscreen. Modern advances have created other that do not fit comfortably into these categories of stamp and substrate, including those of electrophotography (xerography) and ink-jet printing [22].

4.1.1   Lithography

It is interesting to start with lithography because of its familiarity to the semiconductor industry. A planographic (flat-surfaced) process, the image is set on a level surface without incisions and contour changes [23]. In the original instantiation of lithography, the image was drawn on a smooth-faced stone in a greasy substance and then the whole stone was dampened with water. The ink rolled onto this stone had an affinity for the greased areas while simultaneously repulsed by the areas covered only by water. In this way a copy of the image in ink could then be transferred to a piece of paper.
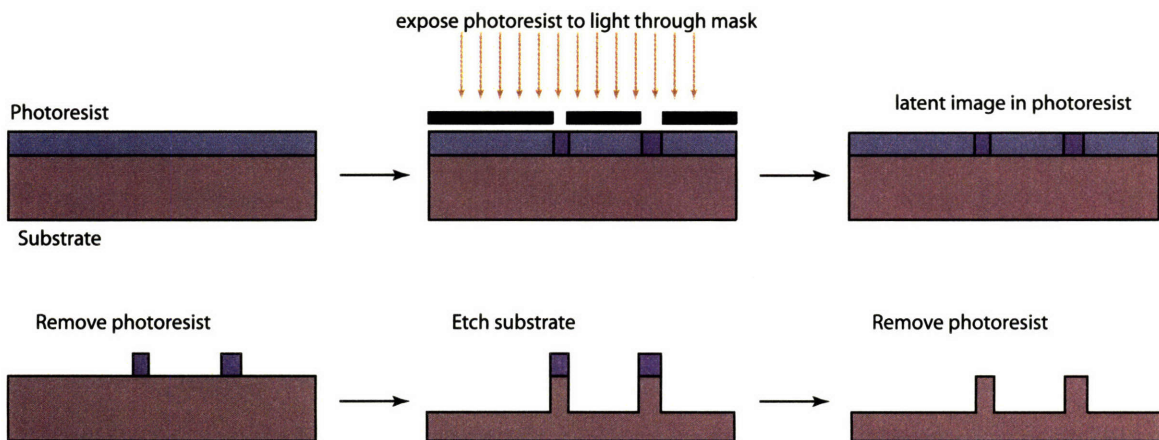
Figure 4-1: Photolithography which is the mainstay of the microelectronics industry is used for patterning silicon as well as other semiconductors and metals.

Lithography in microelectronic device manufacturing is planographic but different in that the image is placed onto the surface (usually that of photoresist) by illumination by light through a mask. The image resides latently in the photoresist, which has reacted to the exposure of light. Subsequently, the photoresist is developed and washed away, leaving either the positive or negative image of the mask. Once this photolithography is performed, the exposed underlying substrate may be selectively

etched due to the protection of the patterned photoresist.

4.1.2 Relief and Intaglio

In contrast, relief and intaglio printing rely on raised and sunken surfaces. Relief printing uses a template in which the desired image extends out from the surface. This template is inked and then pressed against the paper, or desired substrate, and only the extruded areas leave an imprint. Intaglio is the exact reverse, in which the image is dug into the template, etched chemically or physically. These recesses are filled with ink, while the flat surface stays clear of ink, so upon transfer the image is defined by the grooves [23].
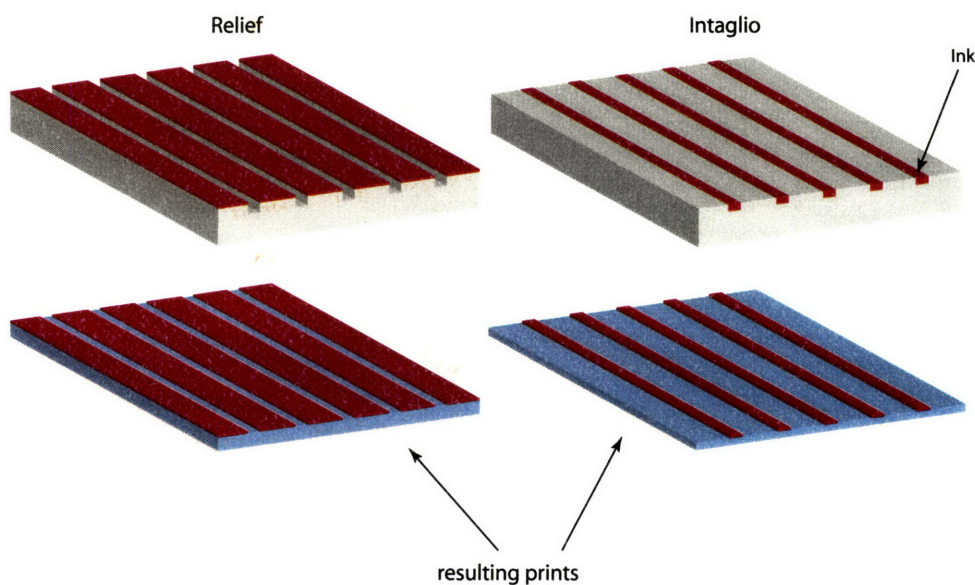
Figure 4-2: Relief and intaglio printing.

4.1.3 Silkscreen

Silkscreen is the method by which ink is pushed through a screen, blocked in places by a stencil in the screen. This method is noteworthy here in that it is similar in principle to shadowmasking. Small-molecules organics, as opposed to polymers, are deposited by thermal evaporation and can be patterned by placing a "stencil" between

37

the source and the substrate. The stencil is called a shadowmask, and is usually made of metal, placed in contact mode with the substrate.
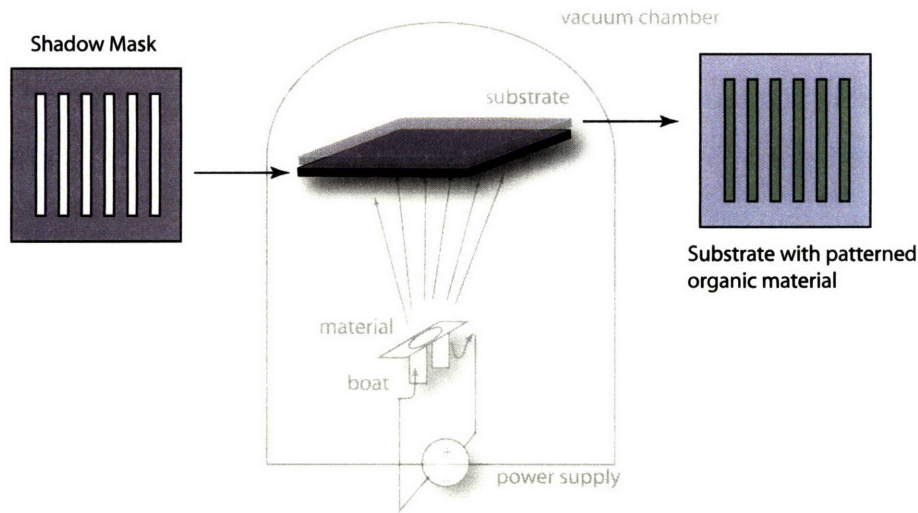
Figure 4-3: Shadowmasking to pattern thermally evaporated organic layers.

4.2 Soft Lithography

4.2.1 Background

Optical lithography, or photolithography, is the most essential, fundamental technique of microfabrication. Almost all integrated circuits are fabricated using photolithography. Nevertheless, there are limitations to photolithography, such as being expensive, poorly suited for nonplanar surfaces, and applicable mainly to just photoresists also motivate the exploration of something like microcontact printing [24]. In our case, the need to work with nontraditional materials is a central reason for pursuing novel methods.

G.M. Whitesides' group started the field of soft lithography in 1993 [25] and developed much of it. For a while, the voiced merits of soft lithography were seated in the idea that photolithography would reach a fundamental barrier in attainable

resolution at around 100nm, unacceptable for an industry that was following the exponential rate of Moore's law [24]. But forecasts for the end of photolithography have repeatedly turned out to be premature. Shorter wavelengths and clever resolution-enhancement techniques have addressed the physical limits set by diffraction, and probably will continue to do so. Regardless, soft lithography has found applicability in numerous ways and its development and use continue unabated.

4.2.2 Microcontact Printing

Soft lithography is so named because it is a set of microfabrication methods that share the feature of using a patterned elastomer as a stamp, mold, or mask. Microcontact printing was the forerunner, and is considered the most representative of the set [26]. Relief patterns are formed in an elastomeric stamp, commonly made out of the material polydimethylsiloxane (PDMS). This is often done by creating a template in a silicon wafer, called a master, which can be reused indefinitely for repeated castings of PDMS (Fig. 4-4). The stamp is then coated with the material to be transferred by various inking techniques, such as immersion or "ink pad"-like pickup. When the stamp is pressed against the substrate, only the relief features come in contact, thereby selectively depositing the ink in those regions. Because the elastomer is significantly deformable, this contact is "conformal" despite nonplanarities of the surface, [24] both on macroscopic and microscopic scales. Often the ink is an SAM (self-assembled monolayer) that can act as a chemical resist on top of a gold substrate, which then undergoes the usual etching steps.

4.2.3 Microtransfer Molding

Other techniques included under the umbrella of soft lithography are variations of molding with the patterned elastomer, such as replica molding, microtransfer molding, micromolding in capillaries, and solvent-assisted micromolding [6]. Molding is the soft lithographic analogue to intaglio methods of traditional printing. In microtransfer molding, the ink material is applied to the stamp where it collects in the depressed
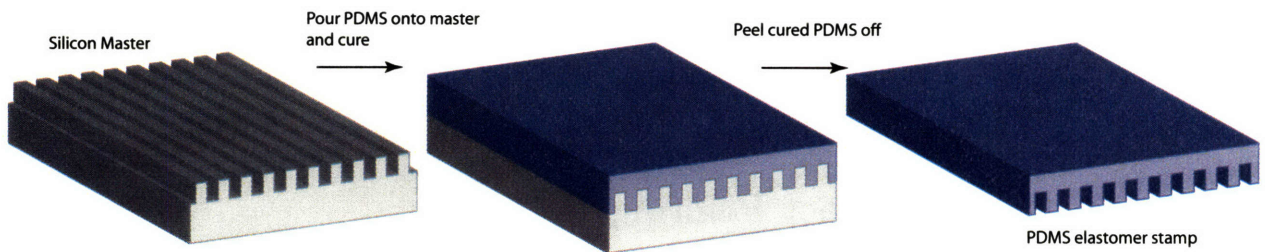
Figure 4-4: Procedure for casting patterned PDMS stamps from silicon masters.
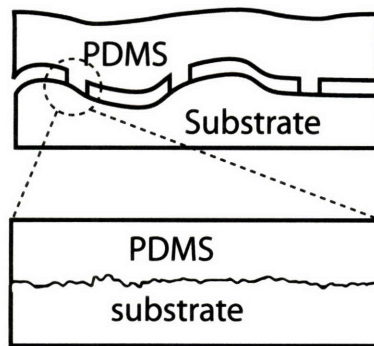
Figure 4-5: PDMS conformally contacts substrates on both the micro and macro level.
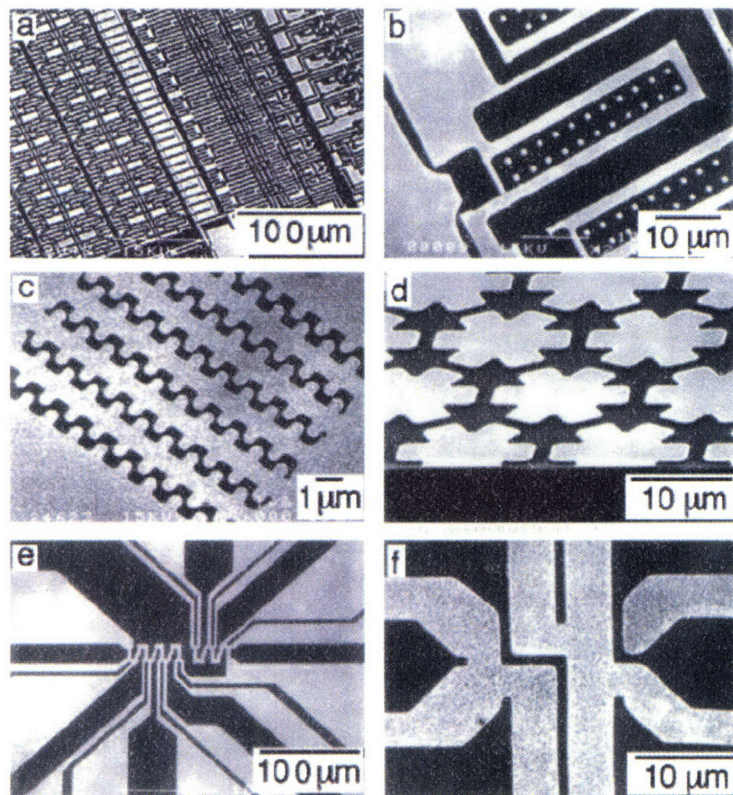
Figure 4-6: Examples of microprinted structures. [6]

features. The excess liquid can be removed by scraping with a flat elastomer block or blowing off with nitrogen, and the final image on the substrate is the complementary of microcontact printing.
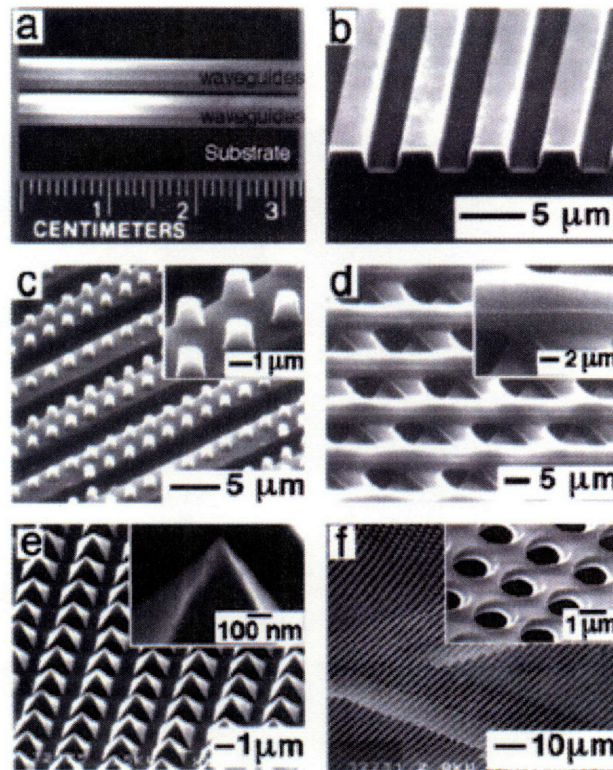
Figure 4-7: Examples of micromolded structures [6].

4.2.4 PDMS

Many different elastomers have been used in soft lithography. These include polyurethanes, polymides, and cross-linked Novolac resin (phenol formaldehyde polymer) [24], but the most commonly used on is poly(dimethylsiloxane).

PDMS contains an inorganic siloxane backbone and organic methyl groups attached to the silicon. Because of its low glass temperature, it is a liquid at room
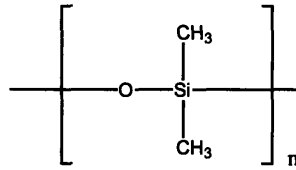
Figure 4-8: PDMS molecular structure[6].

temperature but can be cured into a solid by cross-linking [24]. PDMS has a low interfacial free energy, so many polymers and fluids will not have an affinity to its surface, and it is rather chemically inert. This is both a useful quality in terms of release from template masters and for durability issues, since solvents do not attack the material. However, it is also a problem for the inking step as will be seen in the experimental section.

PDMS is attainable as a commercial kit from Dow Corning, known as Sylgard 184. The liquid silicon rubber base, vinyl-terminated PDMS, and the curing agent, a mixture of platinum complex and copolymers of methylhydrosiloxane and dimethyl-siloxane, are mixed together to form the solid, cross-linked elastomer [6].
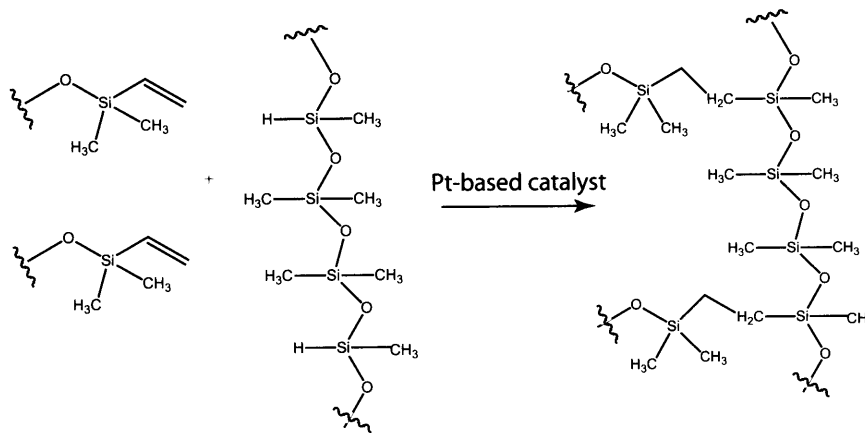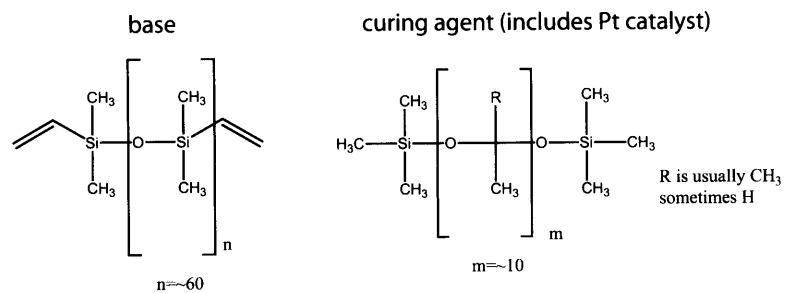
Figure 4-9: Curing mechanism of PDMS and resulting cross-linked elastomer. [7]

Chapter 5

Stamped QD Films

There are two reasons for pursuing stamping of quantum dot films: improving the quality of deposition and enabling patterning. Last chapter, we discussed the two methods of microcontact printing and microtransfer molding (micromolding) for patterning. In this section, we discuss why we seek a new method to deposit quantum dots. Then we show that quantum dot solutions do not work well with PDMS, unless the PDMS is given a surface treatment.

5.1 Background: Phase Separation

The phase separation method for forming monolayers of quantum dots significantly improves the device performance over that of any other previous demonstration of a QD-LED. However, the spin-cast method is unoptimal because it necessarily couples the deposition of the underlying organic layer and the quantum dot layer. This constrains the organic material to be solvent compatible with quantum dots. In addition, the purity of the organic layer is compromised in this technique due to contact with impure solvents. A major advantage of thermal evporation is the high purity of materials that can be deposited solvent-free. In the phase separation method, the small molecule organic comes in contact with the organic solvent, since the QD/organic molecules are spin-cast out of solution.

The phase separation method is also inherently a blanket deposition, with no

capability for defining patterns. And a QD film cannot be patterned using standard techniques. Lithography with photoresist is unsuitable because quantum dots are a unique material set. They are often inhomogeneous balls composed of more than one semiconductor material as well as an organic capping. It would be difficult to devise an etch recipe that could remove exposed quantum dots after a photoresist exposure in a consistent, controllable manner. Removing the photoresist afterwards without destroying the underlying quantum dot layer would also be an issue. A QD film is not one dense solid that is automatically attached to the underlying bulk, like most other semiconductor films used in lithography. It is more like a loose spread of particles lying on top of a surface and therefore easily damaged if an overlying layer of resist were to be pulled off it.

One other consideration is that in a QD-LED, the quantum dots often lie on top of small molecule organics which are highly susceptible to solvent exposure necessary in lithographic processes. In patterning an all-organic device, the sensitivity to solvent degradation is bypassed since patterning simply requires vapor phase deposition through a shadowmask. This technique is unusable for quantum dot patterning, because size and composition prevent growth techniques like thermal evaporation and sputtering, therefore precluding shadowmasking as an option.

5.2   Microtransfer Molding (Micromolding)

When the quantum dot/chloroform solution is inked onto patterned PDMS, the quantum dots end up exclusively in the trenches of the stamp. Therefore, the patterned film that results from stamping the PDMS onto a substrate is that of microtransfer molding (or micromolding). An interesting observation is that micromolding occurs because the quantum dot solution does not wet the PDMS well.

The easiest way to show the poor wetting is dropcasting on a flat, unpatterned PDMS stamp. The solution does not spread evenly on the surface, but rather balls up. As solvent evaporates away, the balled up solution shrinks into a smaller ball. The surface tension at the edge of the shrinking droplet is strong enough to pull

in quantum dots along with the solution, leaving nothing behind on the PDMS. This continues until the solvent is fully evaporated, leaving behind very concentrated clumps of quantum dots in localized areas. Spincasting spreads the dots out more evenly across the micron scale (Fig. 5-1 & Fig. 5-2), but produces a film that lacks the smoothness of a film deposited with the phase separation technique.
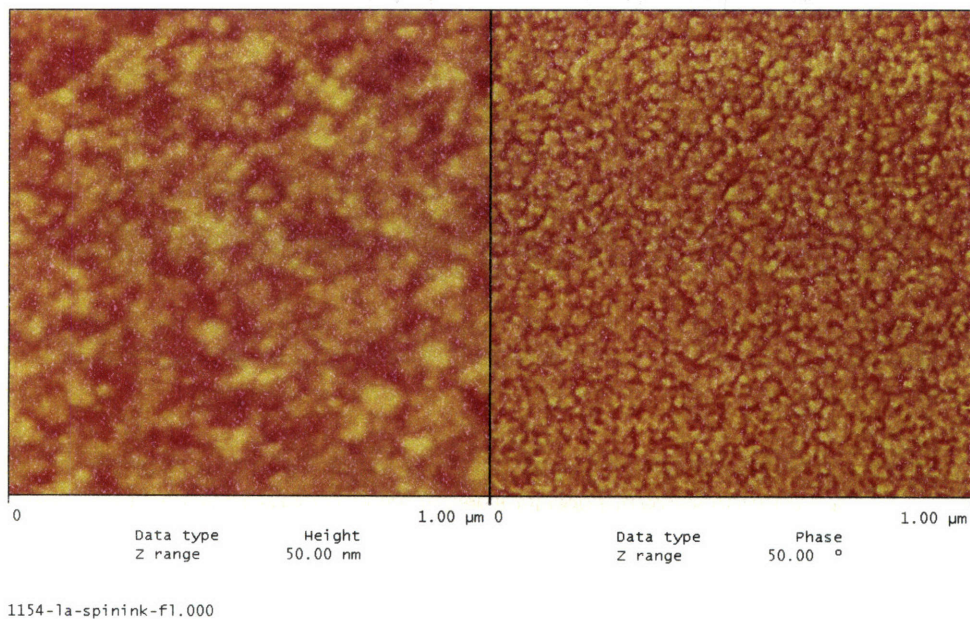
Figure 5-1: Printed quantum dot film from spincasting on a flat PDMS stamp.

The surface tension dynamics of the drying chloroform/dot droplet is more useful with patterned stamps. As the solvent edge moves across the PDMS substrate, it pulls the dots along until they fall into a trench. Because of this action, the crude technique of dropping solution onto patterned PDMS can give remarkably well defined patterns of dots (Fig. 5-3). However, micromolding does not easily lend itself to monolayer formation. The amount of quantum dots that falls into a hole is not controllable, and prevents consistency from clump to clump. By creating a PDMS stamp with recesses that are precisely the depth of the quantum dot diameter, a uniform, monolayer pattern could in princple be achieved. However, the crux of quantum dot technology is the size-tunability, so for any given solution of quantum dots of a specific size, a
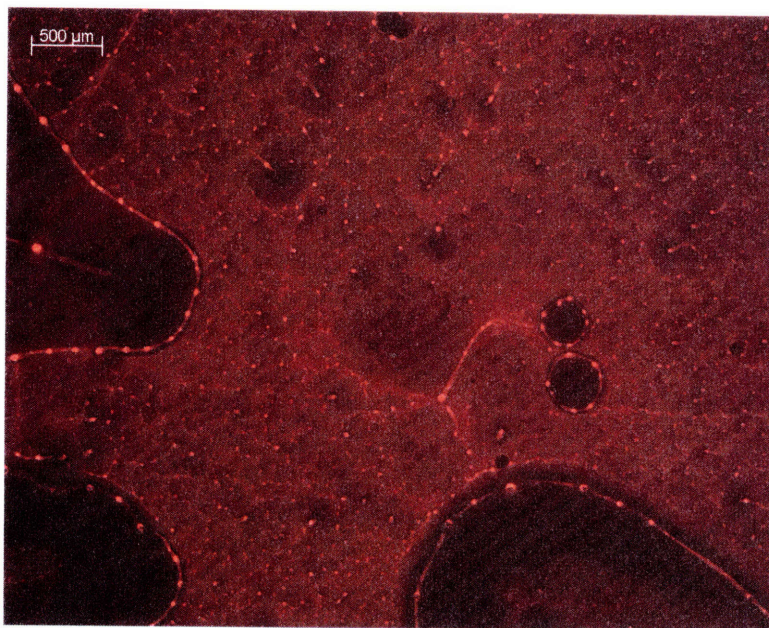
Figure 5-2: Photoluminescence optical microscope photo of a film printed by spincasting on a smooth surface of PDMS. Nonuniformity is visible on the micron scale.

new master tailored to it would need to be fabricated.

5.3 Improving Surface Kinetics of the Stamp

5.3.1 Surface Wetting

Microcontact printing would be a better solution, because it would not depend on the depth of the features in the stamp. If the spreading properties of the chloroform/dot solution could be improved, a monolayer film could be formed on the relief features of a stamp by spincasting the solution. To improve spreading properties, an examination into the basics of wetting and surface energies is helpful.

A drop of a chloroform/dot solution forms a high contact angle when placed on the PDMS stamp (Fig. 5-5). The tendancy for the solution to ball because of unfavorale interfacial energies translates to poor spreading properties. This in turn degrades the quality of the printed ink film.

0		4.00 µm
Data type	Height	
Z range	50.00 nm	

0		4.00 µm
Data type	Phase	
Z range	60.00 °	
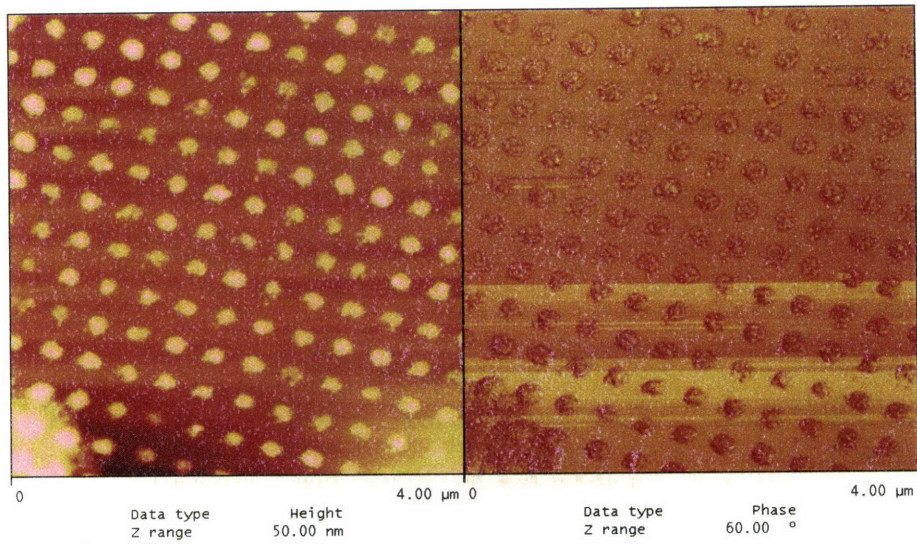
Figure 5-3: AFM of molded quantum dots in a period pattern of circles.

0		4.00 µm
Data type	Height	
Z range	93.55 nm	

0		4.00 µm
Data type	Phase	
Z range	50.00 °	
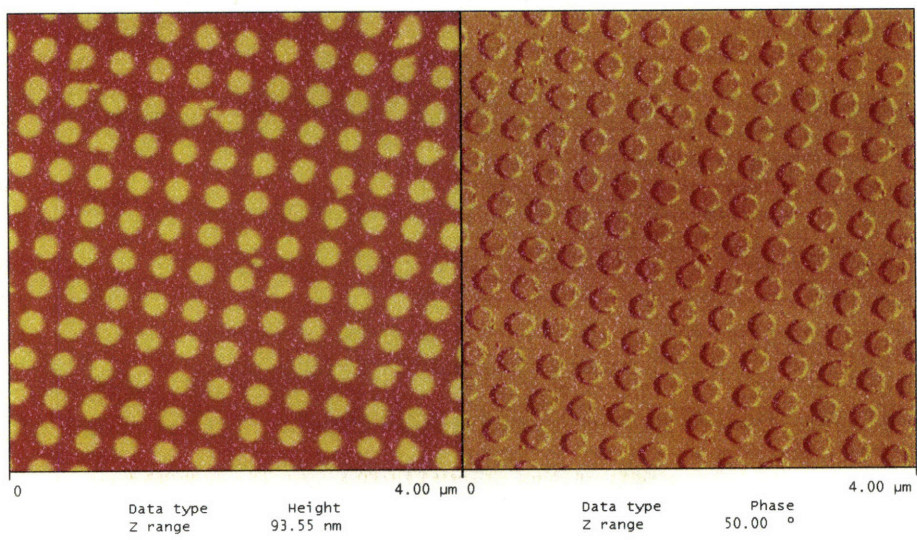
021104-pattern1.000

Figure 5-4: AFM of the silicon masters from which the stamps were made.
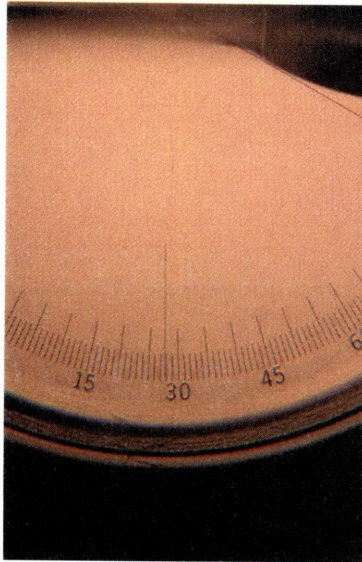
Figure 5-5: Contact angle of a chloroform droplet on PDMS.
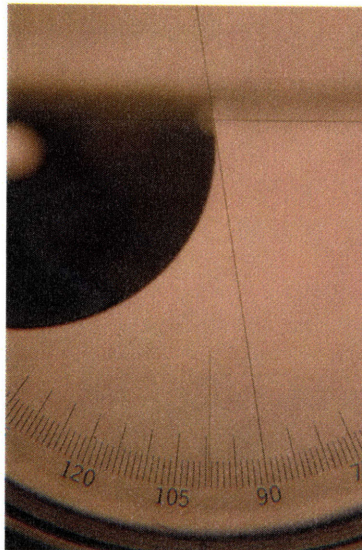
Figure 5-6: Contact angle of a water droplet on PDMS as a reference point.

5.3.2 Surface Energy

Wetting properties are determined by surface or interfacial energies. When a drop of liquid is formed, surface tension is responsible for its curvature. The amount of surface tension depends on the excess energy available due to unbalanced interatomic forces on molecules at the boundary. Within the bulk of the liquid, the molecules are naturally bonded in optimal formation that balances forces out. At the boundary, this optimal formation is not possible due to missing neighbor molecules. To achieve equilibrium, the excess, unbalanced cohesive forces must exert more strongly on the remaining neighbor molecules still there, creating surface tension.
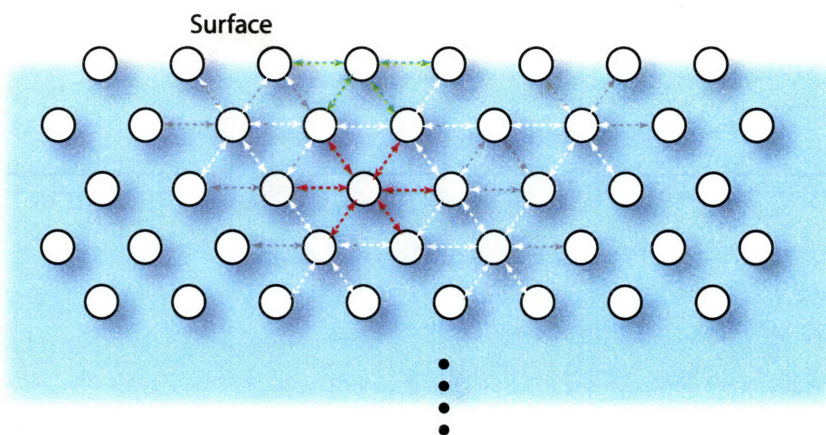
Figure 5-7: Intermolecular forces balance out in the bulk of a liquid. But at the surface, lack of neighboring molecules cause an imbalance and greater forces between the molecules present.

Sometimes if the liquid is placed on a solid, the attractive forces between the liquid molecule and the solid molecule can overcome the forces between the liquid molecules. The degree to which this adhesion occurs controls the wettability of specific solid by a specific liquid.

The relationship of the liquid drop on the solid is given by the Young-Dupré Equation [27]

$$\gamma_{SV} - \gamma_{SL} = \gamma_{LV} cos\theta \qquad (5.1)$$

γ_{SV} is the surface tension of the solid, γ_{LV} is the surface tension of the liquid, γ_{SL} is the solid-liquid interfacial tension, and theta is the contact angle. Rewriting the equation

$$cos\theta = \frac{\gamma_{SV} - \gamma_{SL}}{\gamma_{LV}} \qquad (5.2)$$

Differentiation between wettability and unwettability is commonly assigned to 90°. If the contact angle is anywhere from 0° to 90°, the liquid is said to wet the substrate, and not to wet the substrate if the contact angle is between 90° and 180°.

>90°   =90°   <90°
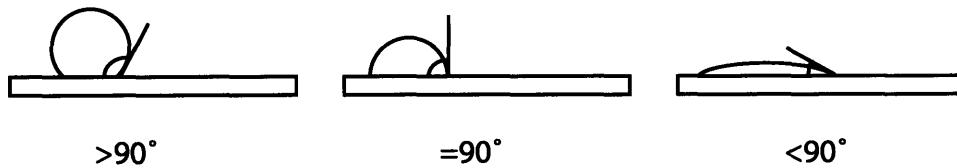
Figure 5-8: The lower the contact angle, the better the liquid is said to wet the substrate.

Since the units of gamma are [energy/area], a "change in energy" equation of a droplet wetting the surface of a solid can be written as

$$\delta E = \gamma_{LV} \cdot \delta A_L + \gamma_{SL} \cdot \delta A_S - \gamma_{SV} \cdot \delta A_S \qquad (5.3)$$

δA_S and δA_L are the change in surface area of the solid exposed to vapor and the change in surface area of the liquid. This equation describes the event of increased liquid surface area and liquid-solid interface surface area and decreased solid surface area due to the spreading of the liquid (Fig. 5-9). In a simplistic approximation of a flat droplet, A_L and A_S are approximately equal. Therefore,

$$\frac{\delta E}{\delta A_S} = \gamma_{LV} + \gamma_{SL} - \gamma_{SV} \qquad (5.4)$$

Area of drop that wets better minus the area of original drop

Area of solid exposed to air

Also, area of solid no longer exposed to air

Area of original drop

Substrate
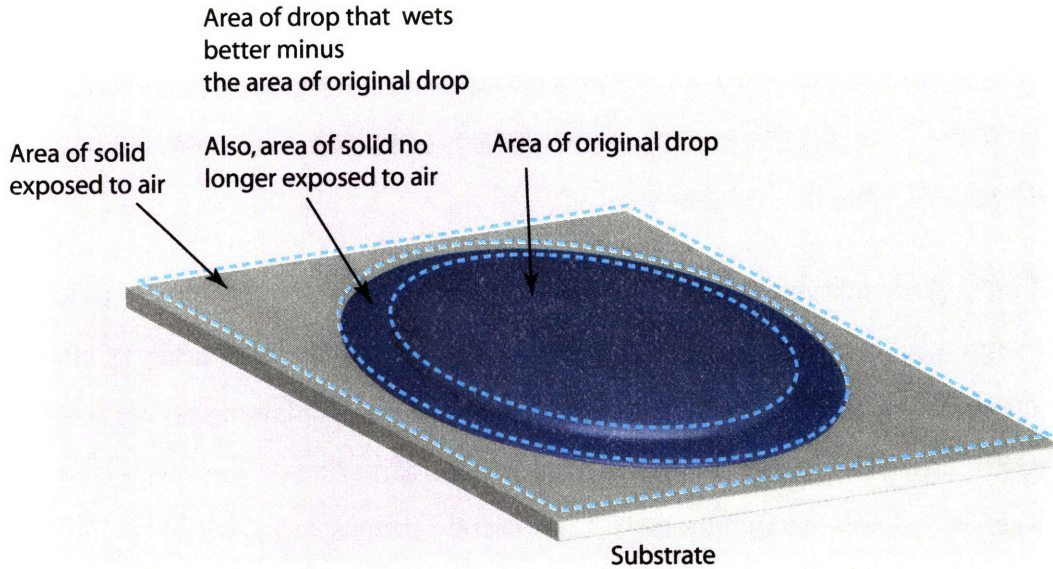
Figure 5-9: Figure of the different surface areas.

For the wetting to be able to occur spontaneously, the change in energy must be negative indicating a relaxation in the system. This means the right-hand side

$$\gamma_{LV} + \gamma_{SL} - \gamma_{SV} < 0 \qquad (5.5)$$

This inequality indicates that wetting is aided by lower liquid surface energies (low surface tensions), low interfacial forces between the solid and liquid, and high solid surface energies. In examining the initial Eqn. 5.1, striving for a low contact angle also yields the same result. A low contact angle means $\cos\theta$ is as close to positive one as possible. To ensure a positive right-hand side, γ_{SV} should be large, while γ_{SL} small. And to achieve the highest possible value towards one, the denominator γ_{LV} should be small [28] [29]. In other words, better surface wetting occurs with higher surface tension of the solid, lower solid-liquid interfacial tension and smaller surface

tension of the liquid.

5.3.3 Low Surface Energy of PDMS

One of the reasons often cited for PDMS being an excellent material for microcontact printing is its low surface energy. This translates to easy release from a master template, as well as chemical inertness with respect to solvents it comes in contact with. As Dow Corning, the major commercializer of PDMS, states as to what makes silicones special [30]:

> The organic portion in poly(dimethylsiloxane) or PDMS – by far the most common silicone polymer – is the methyl group. The surface energy of any substance is a direct manifestation of the intermolecular forces between molecules. In the case of the methyl group, these forces are almost the weakest possible (only aliphatic fluorocarbon groups are lower).
>
> The inorganic siloxane backbone is the most flexible polymer backbone available. This allows the methyl groups to be arranged and presented to their effect. Consequently, PDMS provides one of the lowest-energy surfaces known. This results in a low-surface-energy polymer that can be bettered only by more expensive fluorocarbon polymers.

The surface free energy of PDMS is listed as 22 mJ/m^2, roughly the same as the critical surface tension value of methy groups (22-24 mJ/m^2) [31].

5.3.4 Improving Interfacial Energy

From the elementary understanding of wetting presented above, there are a few ways to atempt improved wetting. One way is to increase γ_{SV}, which means changing PDMS for a material with a higher surface energy. However, because of the convenience, benefits and familiarity of PDMS as the most widely commercialized and standard elastomer, the option of substituting for alternative elastomers is unattractive. Another option is to reduce γ_{LV} by finding a liquid solvent with a lower surface

tension. But many of the common solvents have values similar to chloroform, as seen in Table 5.1.

Solvent	Surface Tension (dynes/cm)
Acetic Acid	28
Acetone	24
Benzene	29
Chloroform	27
Ethyl Alcohol	24
Ether	17
Hexane	18
Isopropyl Alcohol	22
Toluene	29
Water	73

Table 5.1: Surface tension of various common solvents at room temperature.

An attempt to use hexane, which also solvates quantum dots, shows that perhaps the amount of gain to be had by substituting different solvents with rather similar surface energies is small, and resulting films are similar to that of spincasting with chloroform.

In deciding to keep the elastomer material and the solvent type unchanged, the remaining option is to use surface modifications. A common technique with PDMS is to use UV ozone or oxygen plasma, which has been shown to turn the surface hydrophilic.
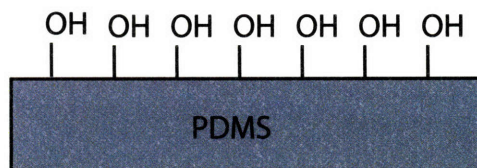
Figure 5-10: Oxygen plasma and UV ozone treatments make the surface of PDMS have a higher surface energy because of the chemically reactive OH groups.

Wetting appears to improve on PDMS treated by oxygen plasma. However, the printed film are disappointing (Fig. 5-11. This may be due to physical changes in addition to chemical ones. After being treated, the top surface of PDMS exhibits a brittle, silica-like layer, as well as signs of roughening. The poor film quality may be

attributable to the loss of conformability of the glassy elastomer, in addition to lack of planar uniformity.
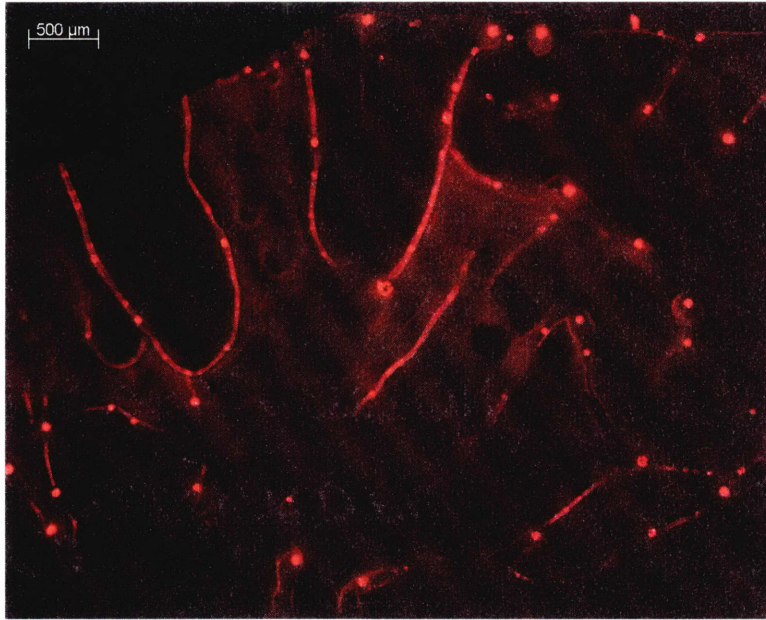
Figure 5-11: Photoluminescence optical microscope photo of a film printed by spincasting on a an oxygen plasma treated PDMS surface. Nonuniformity is visible on the micron scale.

An adhesion layer made up of a completely separate material turns out to work better. Parylene is a thermoplastic polymer that is deposited by vapor deposition, resulting in a soft, conformal coating. Although it is also considered a hydrophobic, low surface energy material, parylene-C includes a chlorine atom at every phenyl group, and is therefore a slightly more polar variant. It is possible that parylene-C is more attractive to the chloroform solution, effectively increasing γ_{SL}, which allows for a smaller contact angle and better wetting (Fig. 5-12 while still retaining a pliable, smooth surface.

5.4 Microcontact Printing

By parylene-C coating the surface of the PDMS stamp, microcontact printing of quantum dots out of a chloroform/dot solution is possible because of improved surface wetting. The solution of quantum dots is spincast on the parylened PDMS surface,
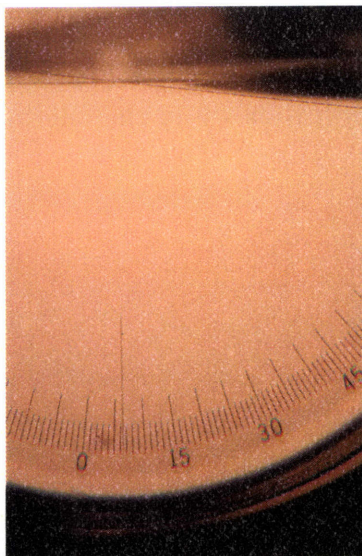
Figure 5-12: Contact angle of a chloroform droplet on parylened PDMS.
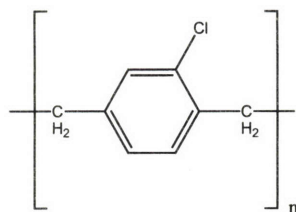
Figure 5-13: Molecular structure of parylene-C.

and because of good spreading, a neat monolayer of quantum dots forms everywhere. AFMs of unpatterned stamped films and patterned stamped films show well-ordered, near monolayer QD films. With parylene coated stamps, printing quantum dots is possible on ITO and a variety of organics (Figs. 5-14, 5-15, 5-16). Printing on a silver film has also been demonstrated, although it is more difficult to get a well-ordered full monolayer (Fig. 6.2). It appears the flatter and smoother the substrate, the better the print quality. Figs. 5-18 & 5-19 show a patterned circle of quantum dots on TPD. Other successful pattern prints are shown in the following chapter on devices.
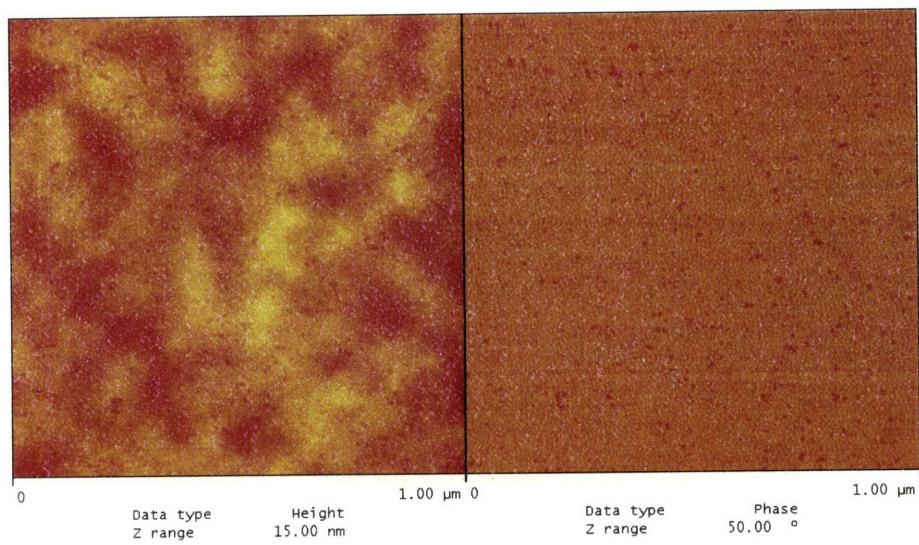
Figure 5-14: Microcontact printed film of CdSe quantum dots on CBP.
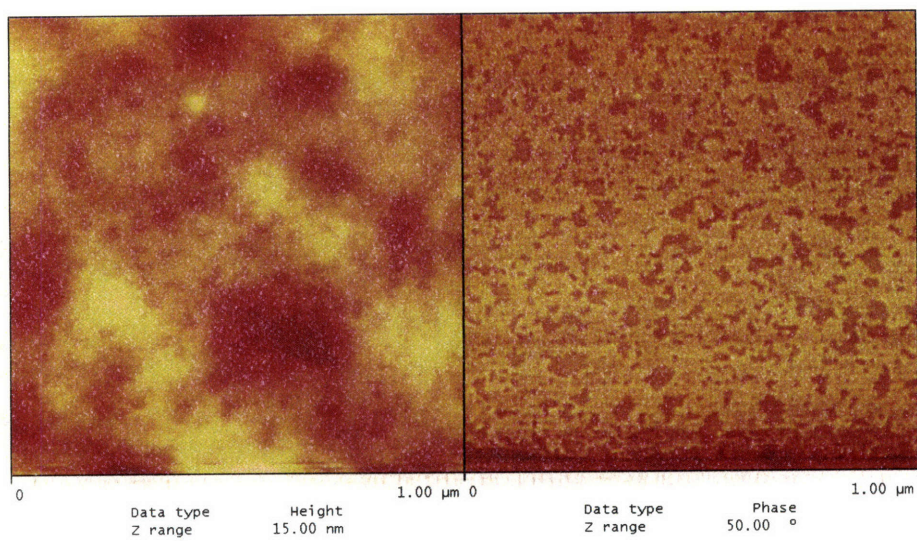
Figure 5-15: Partial monolayer microcontact print of QDs on CBP.
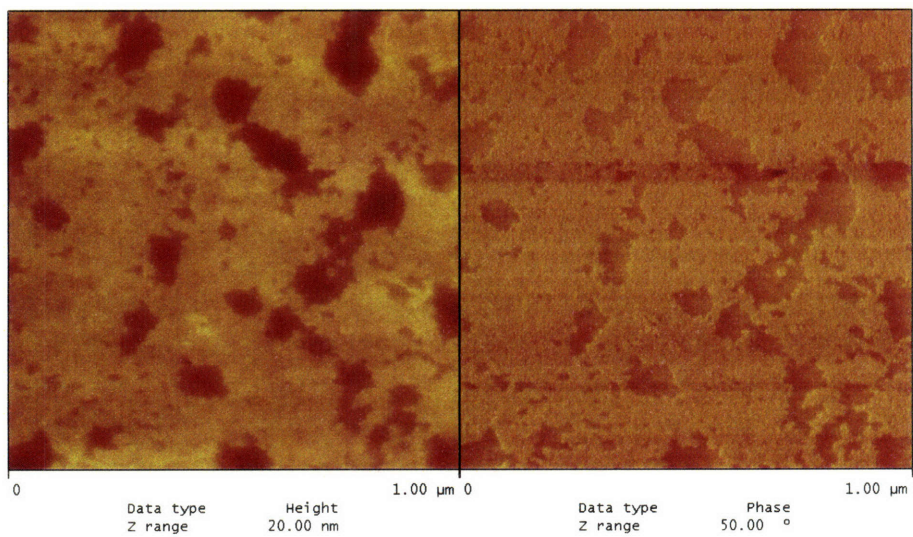
Figure 5-16: Partial monolayer microcontact printed film of quantum dots on TPD.
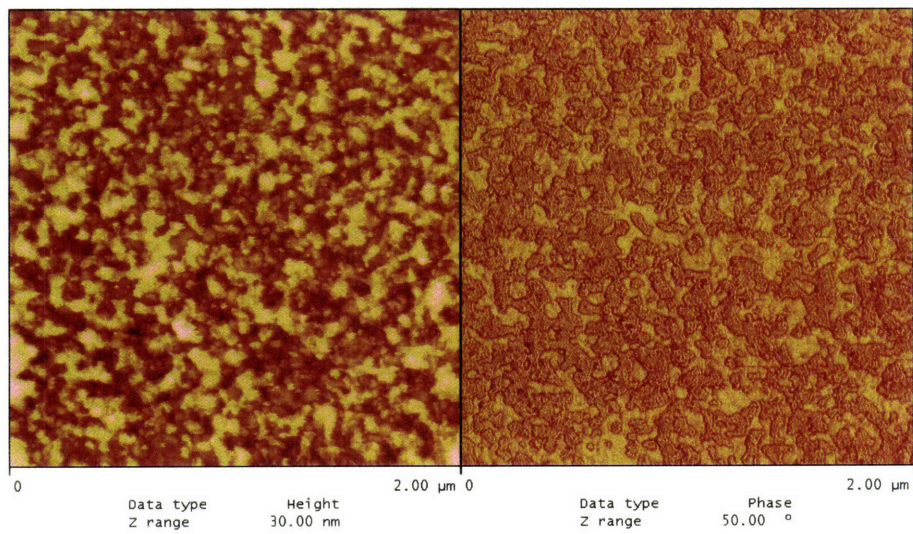
Figure 5-17: Partial monolayer microcontact printed film of quantum dots on Silver.

Data type   Height   Data type   Phase
Z range   50.00 nm   Z range   50.00 °
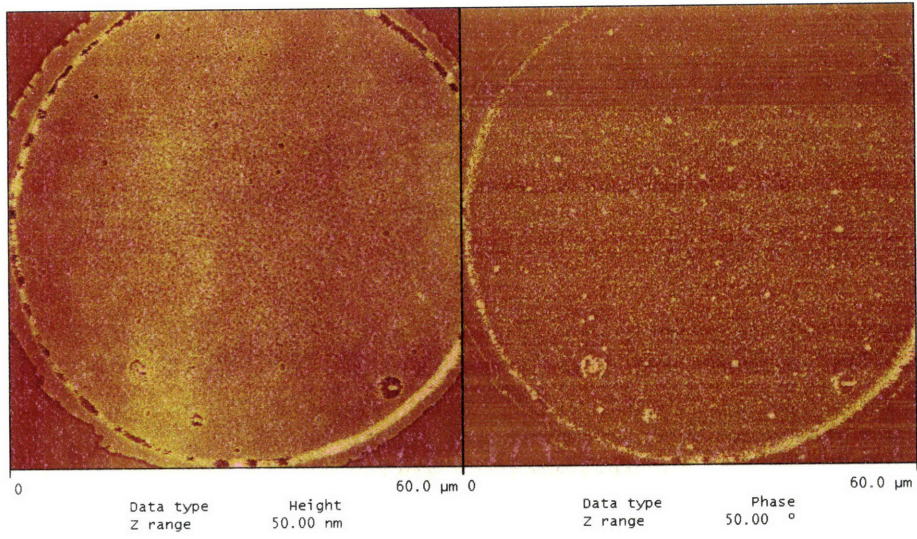
Figure 5-18: Microcontact printing of 60μm large circles.

Data type   Height   Data type   Phase
Z range   50.00 nm   Z range   50.00 °
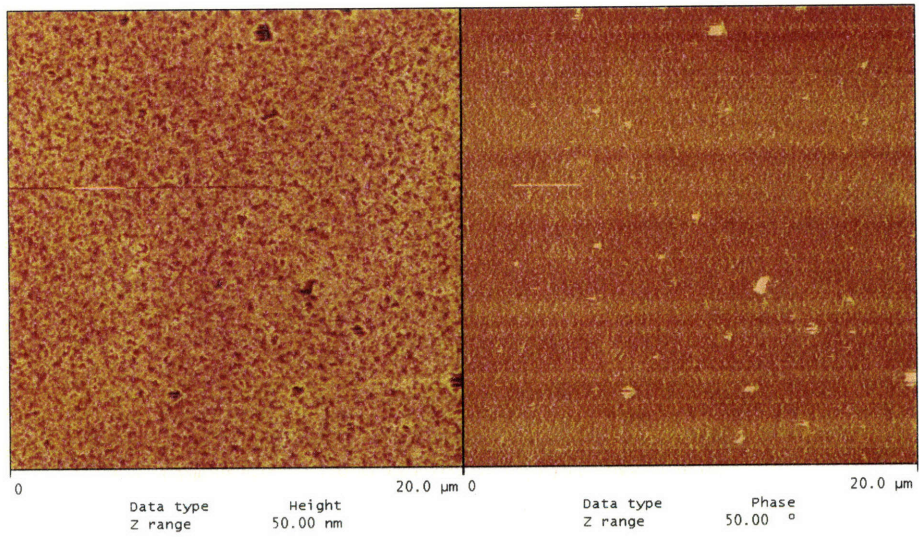
Figure 5-19: Close-up AFM of the circle.

Chapter 6

Device

The demonstration of microcontact printing of quantum dot monolayer films proves the capability to independently deposit quantum dots without the organic molecules, as well as the capability to pattern the quantum dots. The resulting morphology of the microcontact printed films are similar to that of previous phase-separation method, with a densely packed monolayer over a sizeable area. These microcontact printed QD films are incorporated into the same device structure as the phase-separated monolayer devices discussed back in Section 3.3.2 Fig. 3-5, except that the underlying organic molecule is thermally evaporated just like the other organic films in the device, allowing for a higher purity layer.

6.1 Device Performance

6.1.1 I-V and Quantum Efficiency

The current-voltage curves (Fig. 6-2) of the devices are similar to those made by the former phase-separation method. The noise floor of the measurements is around 1×10^{-8} A/cm^2. From roughly 0 to 3V, the devices exhibit ohmic behavior. Above the turn-on voltage of 3V, the device shows space-charge limited conduction with traps, with a voltage to the power of 8 dependence. Unfortunately, an in-depth exploration of possible trap distributions and charge conduction mechanisms is beyond the scope

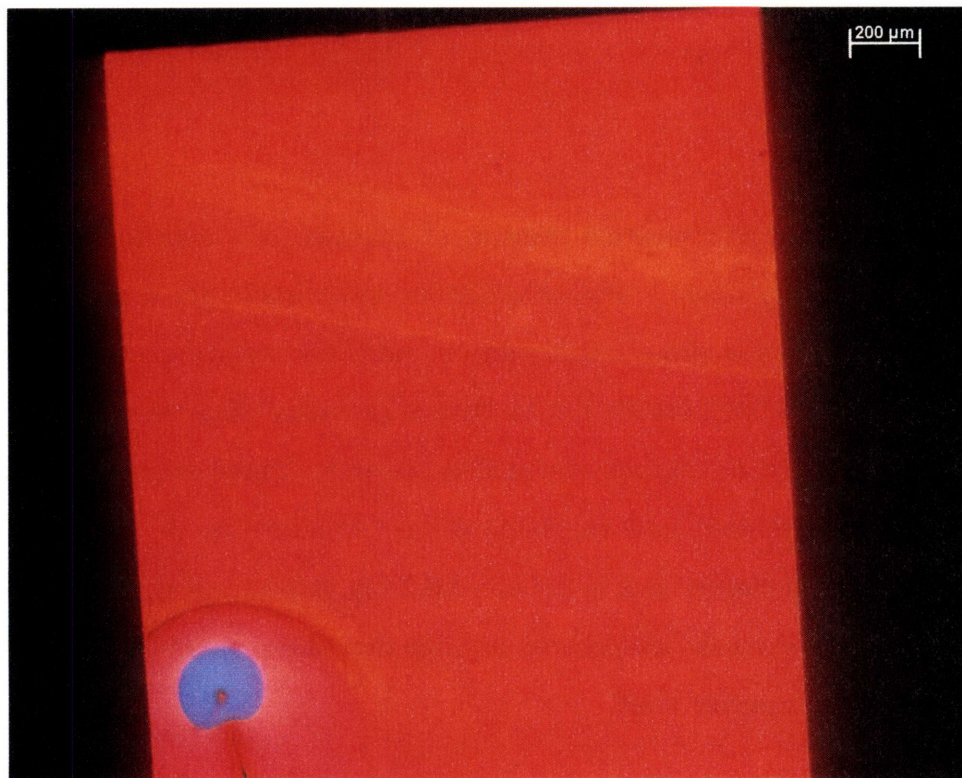**Figure 6-1:** Device with microcontact printed red QD film, showing good large area uniformity and coverage on the scale of the device. The blue spot in the lower corner shows a defect in the stamped QD film, allowing the organic TPD emission to be seen.
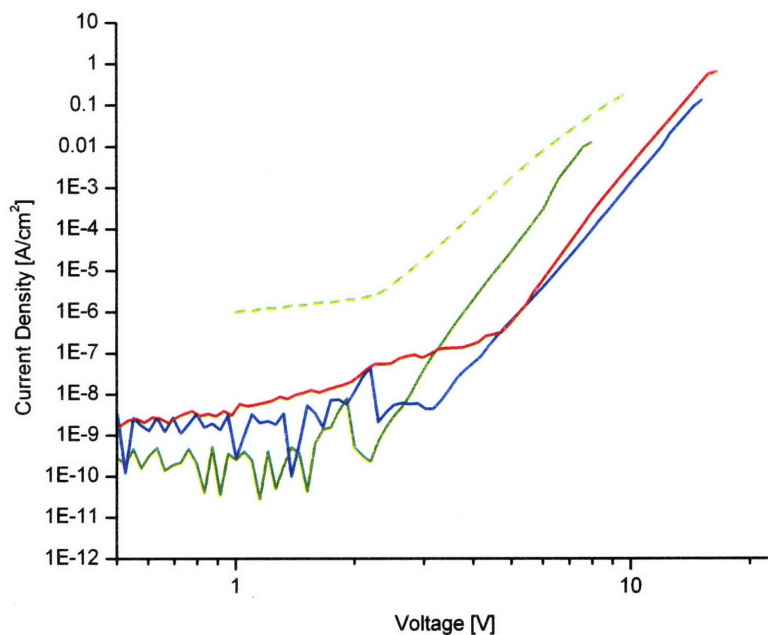
Figure 6-2: IV curves for LEDs that contain stamped QD films, with colors corresponding to that of QD emissions.

of this work. It is interesting that the turn-on voltages seem fairly constant over all devices, including one marked by the dotted line which was fabricated at a different time and under different conditions from the other three.

The quantum efficiency of the stamped QD devices are comparable to those of the phase-separated devices (Fig. 6-3). The red EQE is 1.2% using QDs with solution photoluminescence efficiencies of 70%, green 0.5% with 40% PL efficiencies, and blue 0.25% with 20% PL efficiencies.

6.1.2 Color

The color saturation of the microprinted devices are improvemed dramatically relative to that of the previous devices. One reason is the higher quality of organic films that are now deposited completely by thermal evaporation. The separation of the quantum dot and organic layer depositions appears to facilitate the isolation of the emissive function to the quantum dots. The spectra of the stamped devices show a high
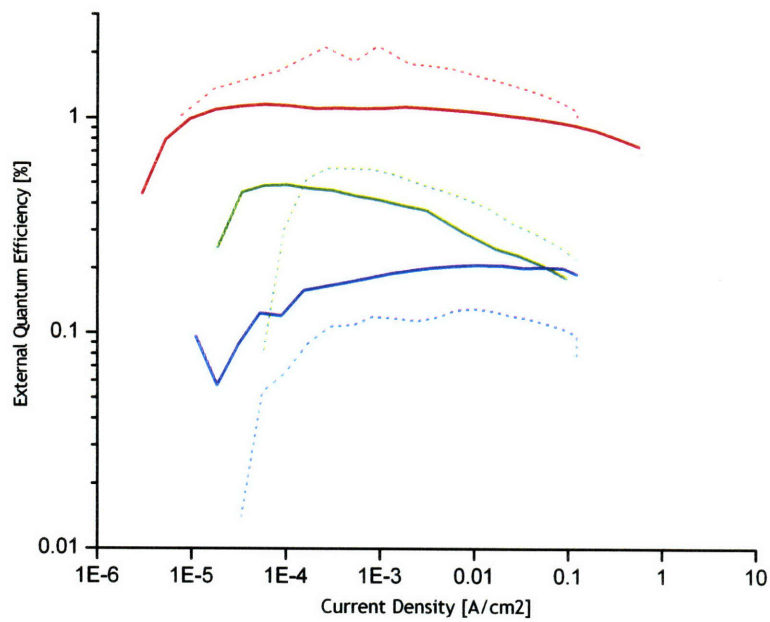
Figure 6-3: Quantum efficiency curves for LEDs that contain stamped QD films, colors corresponding to that of QD emissions. Phase separated QE curves shown as dotted lines.
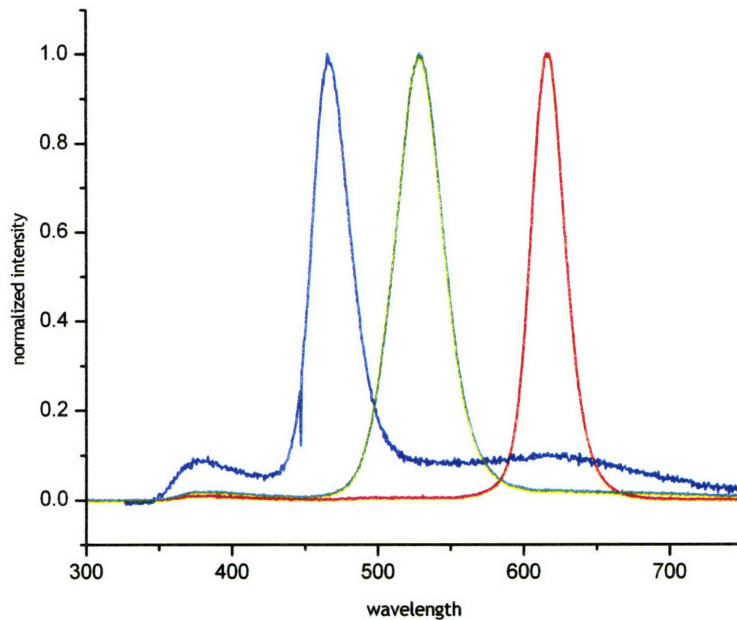
Figure 6-4: Spectra curves for devices that contain stamped QD films.

QD/organic ratio, corresponding to more saturated colors (Fig. 6-4). Improvement also comes from the ability to change the underlying organic layer to CBP, which is not readily soluble in chloroform. It is a wider bandgap material than TPD, giving a greater energy incentive for excitons to transfer from it to the lower energy quantum dots. This is especially critical for the blue dots which have a bandgap energy that is close to that of TPD. Fig. 6-5 shows the CIE coordinates of the stamped and spun phase-separated devices. The stamped devices almost completely enclose the NTSC triangle which defines the colors of CRT televisions.

6.2   Patterned Devices

Substituting the monolayer of quantum dots with a patterned quantum dot film provides the ability to fabricate patterned QD-LEDs. Patterning conveniently requries no additional steps compared to unpatterned device fabrication, aside from the ini-

Figure 6-5: CIE coordinate comparison between stamped and spun devices, and in relation to the NTSC triangle.

tial creation of a silicon master which is reusable many times over. The pattern of circle-patterned QDs shown in Fig. 5-18 gives the electrolu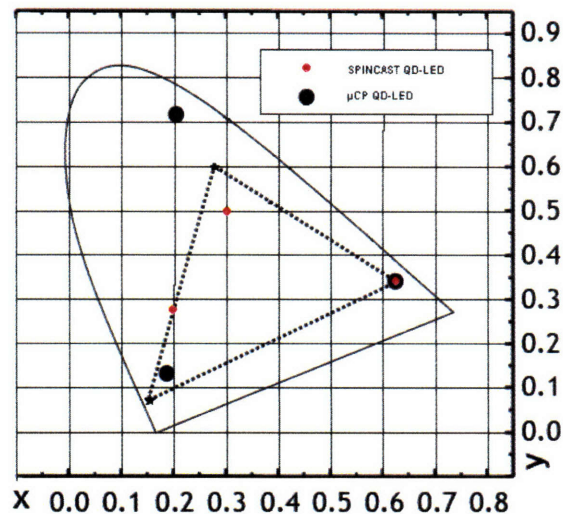minescence pattern shown in Fig. 6-6. It is interesting to note the brightness of the areas outside of the circles. The AFM of the same device (Fig. 6-7) shows that the QD layer there is slightly thicker than a monolayer, while the closeup AFM in Fig. 5-19 shows the layer of quantum dots within the circles are a little sparser than monolayer. The area between the circle's perimeter and the thicker quantum dot layer lacks quantum dots, and in the device photo any organic emission that might be occuring can not be seen. Fig. 6-8 shows an interpretation on how these different regions of the film occurred. Contact does not occur at the edge of the relief pattern, therefore no quantum dots are deposited around the circle. It is energetically favorable for quantum dots to sit at the bottom of a trench instead of sitting on top of the relief surface, making a higher concentration of dots in the trenches likely. If enough deformation occurs that non-relief features touch the substrate, it is possible that the resulting QD layer is thicker at those points.

Fig. 6-9 shows another patterned device with stripe-patterned red quantum dots. The right photo of the device shows it running with higher current, at which it is possible to see the organic emission of CBP between the red quantum dot stripes.
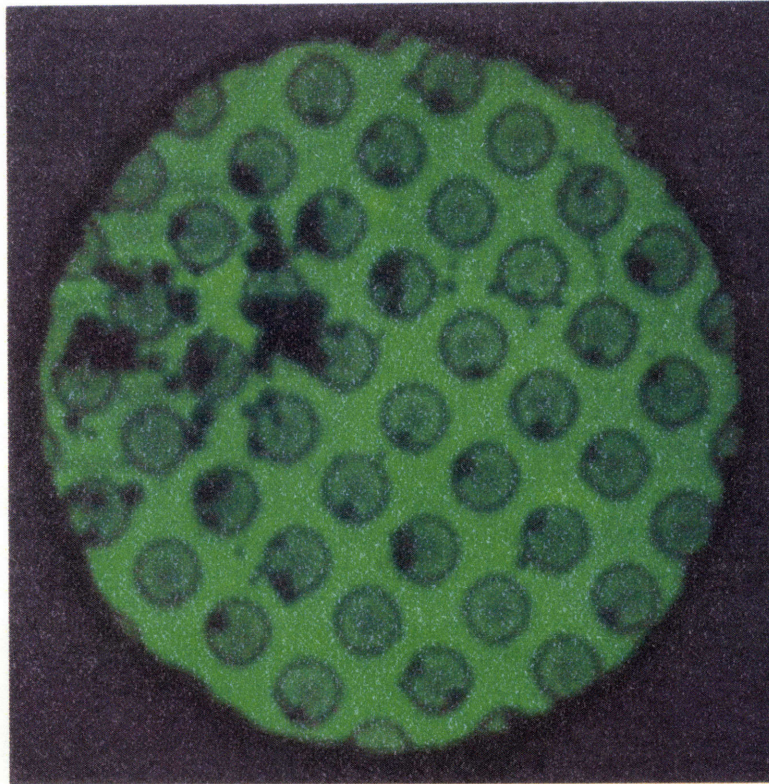
Figure 6-6: Electroluminescence of a patterned green QD-LED device corresponding to the AFM shown in Fig. 5-18 Device is 1mm in diameter.

0	100 µm	0	100 µm
Data type	Height	Data type	Phase
Z range	50.00 nm	Z range	50.00 °
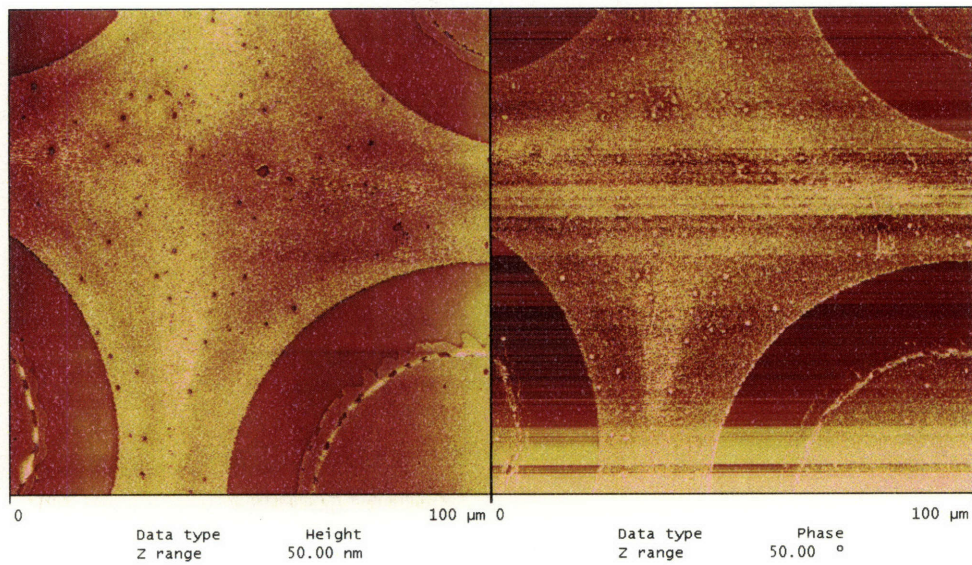
091404-green-stamp-f1.006

Figure 6-7: AFM of the QD circles patterns, offset to show the area between circles.
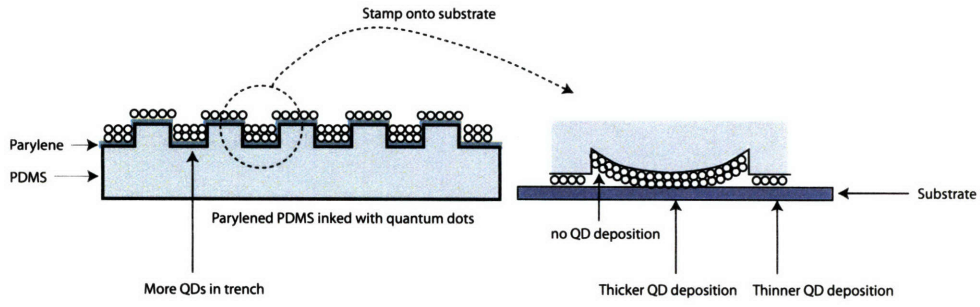
Figure 6-8: Deformation of patterned PDMS that resulted in the QD film shown in Fig. 6-7 due to elastomeric quality of the stamp.

Fig. 6-10 shows the smallest demonstration of quantum dot patterning we recorded.

Figure 6-9: 1mm diameter device showing red quantum dots patterned in stripes. Organic emission visible at a higher operating current, in the right-hand photo.

Fig. 6-11 demonstrates a two-QD color LED, patterned in 25 μm stripes. Lacking registration capabilities, the red and green QD lines were placed roughly perpendicular to each. Where the device lacks quantum dots, the emission is that of TPD. The spectrum of the device is shown in F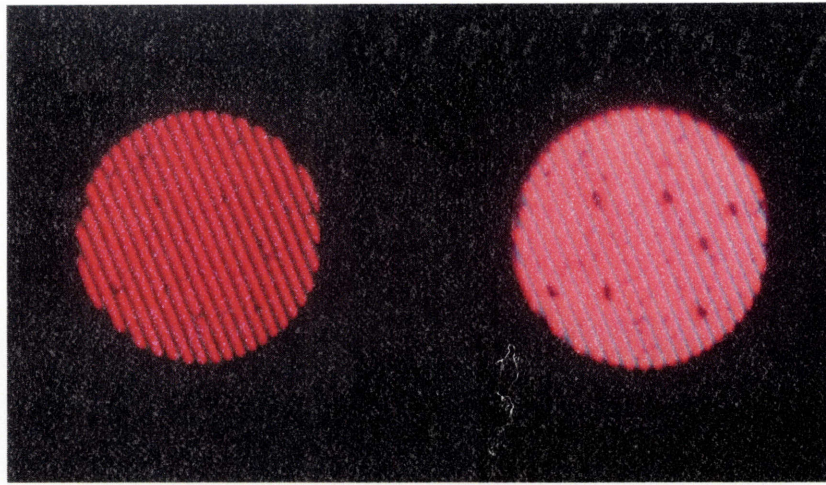ig. 6-12, which shows all three peaks of organic, green QD and red QD. Its CIE coordinate happens to lie at (0.46, 0.41), a whitish-yellow color.

In Fig. 6-13, the corresponding AFM of the QD film, it is interesting to notice in the height image that the edge of the line seems to be thicker than the rest of the QD film. Fig. 6-14 shows a closeup of a patterned QD film, with this edge effect clearly defined. This effect could be caused by the dynamics of a solution spinning on a non-planar pattern or by the distribution of forces at the edge of a pattern when stamping.

It is also important to consider the effects of stamping one type of quantum dot on another, as in the device shown in Fig. 6-11. At the intersection of the lines of green and red quantum dots, there is the question of how charges and excitons are affected
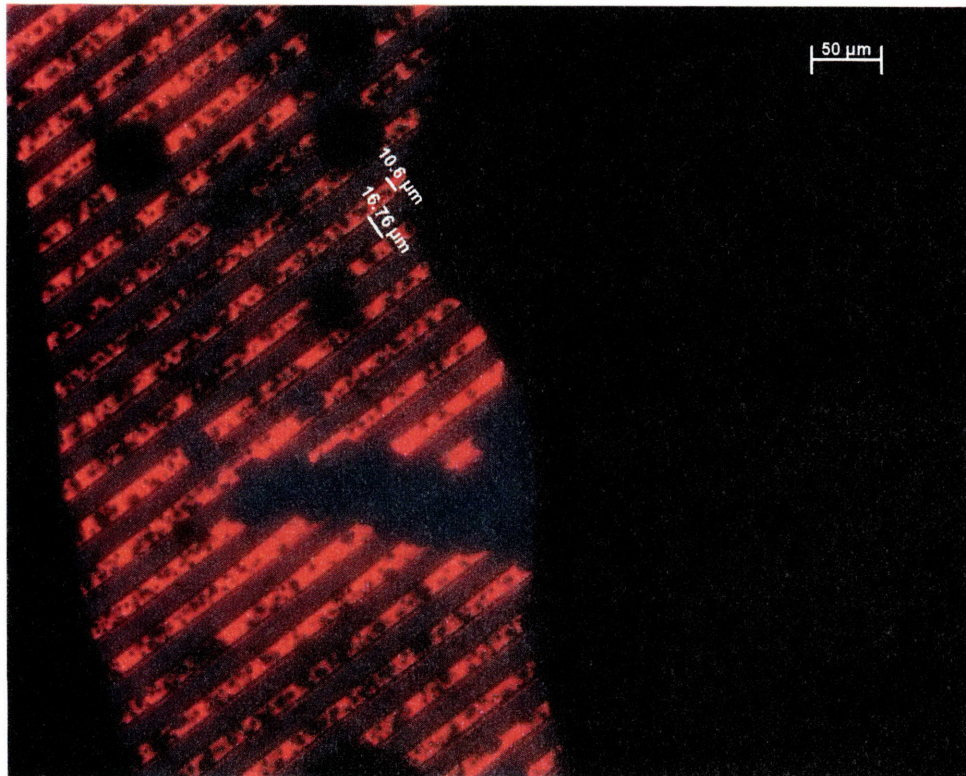
Figure 6-10: A 10 μm line pattern corresponds to a resolution of about 850 dpi for a three color system. The numerous defects are associated with various problems of packaging and isolation from abient conditions.
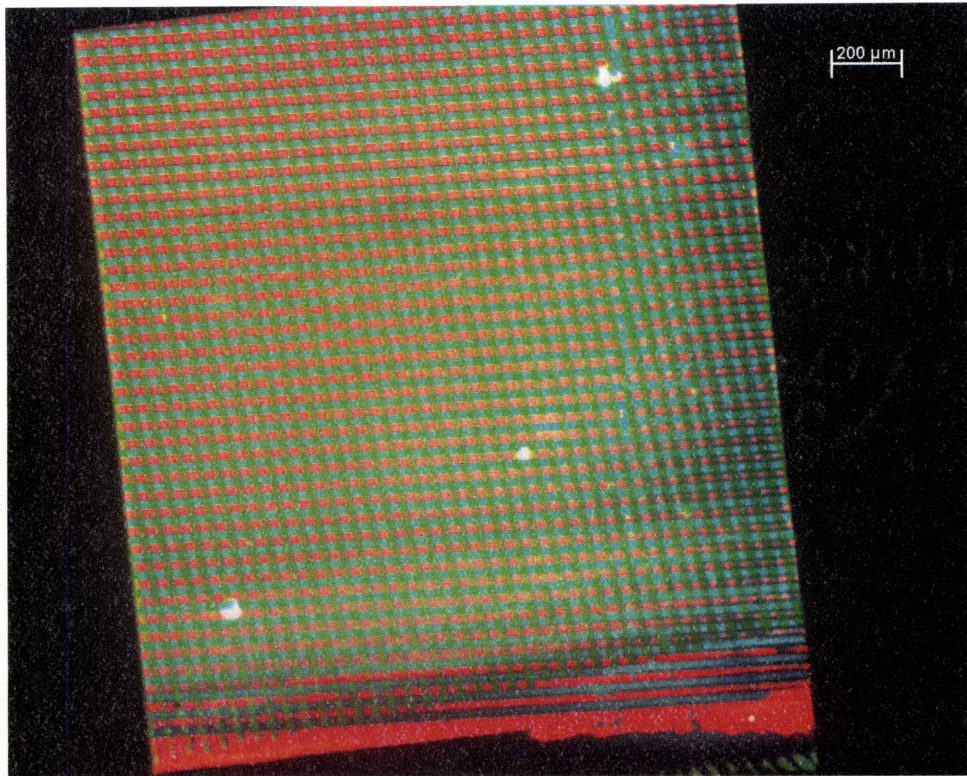
Figure 6-11: Green quantum dot lines printed on red quantum dot lines.
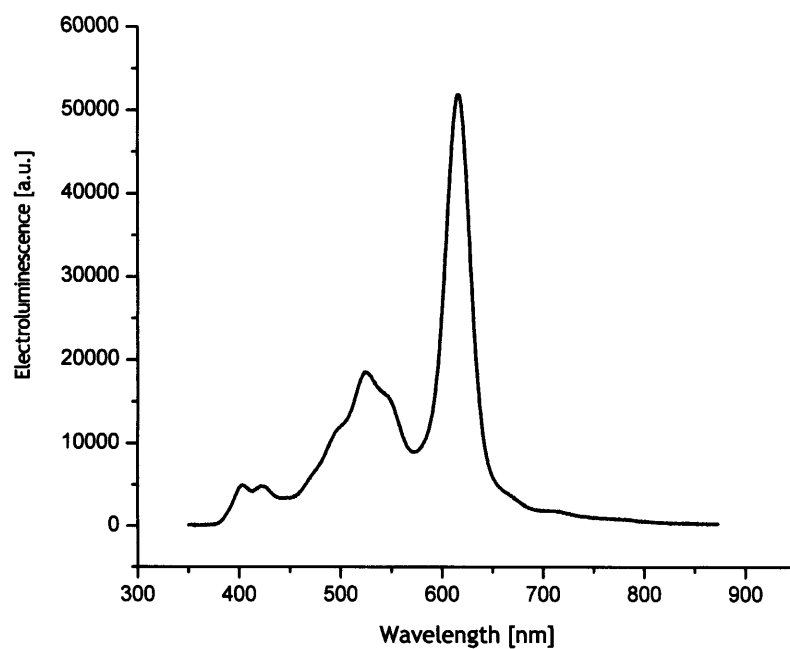
Figure 6-12: Electroluminescence spectra of the device shown in Fig. 6-11. The TPD peak ceneters roughly around 415 nm, the green at 525 nm, and the red at 615nm.

072705-lak-redst-on-grst-f1.003
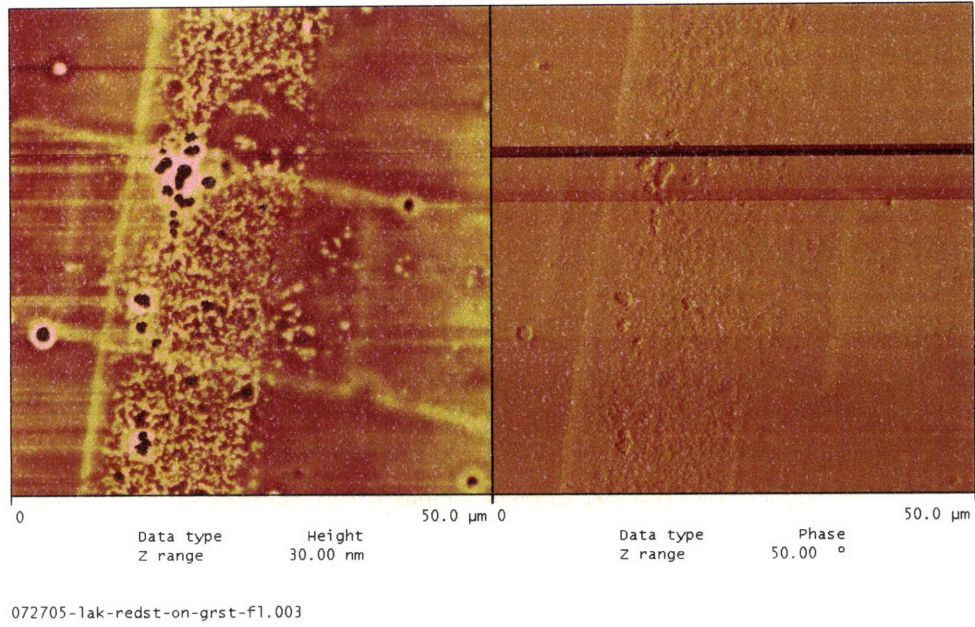
Figure 6-13: AFM of a line of green quantum dots on top of a line of red quantum dots.
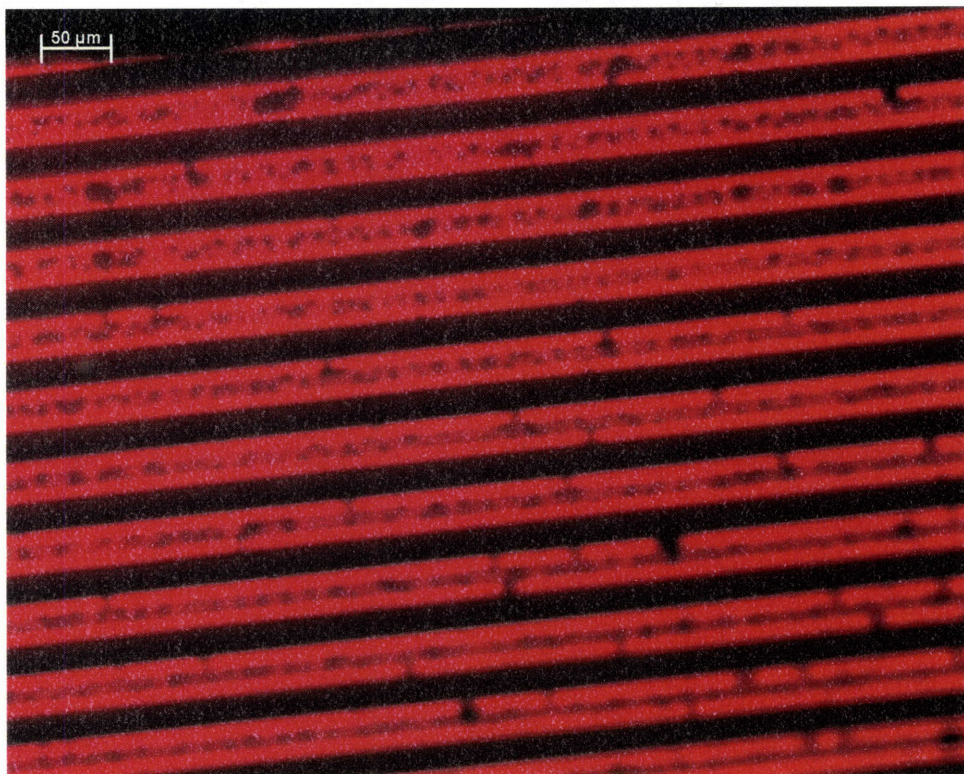
Figure 6-14: Photoluminescence of red quantum dot lines, showing the pronounced edge effect.

by what is essentially an alteration in the device structure and the band diagram of the cross-section. Fig. 6-16 and Fig. 6-18 show devices in which lines of red quantum dots were printed on a full surface print of green quantum dots. Because they have the smallest energy bandgap, the expectation is that it is energetically favorable for exciton relaxation to occur on the red QDs (Fig. 6-17). An initial thought on why instead the red quantum dots that lie on top of green quantum dots seem to barely luminescence is charge trapping. It may be that the red dots trap charge, so that when excitons favorably transfer from the neighboring dots or organics, a radiationless Auger recombination occurs. Or it may be that the electron conductivity of the red dots is higher than that of the holes in the green dots, favoring exciton formation on the green dots.
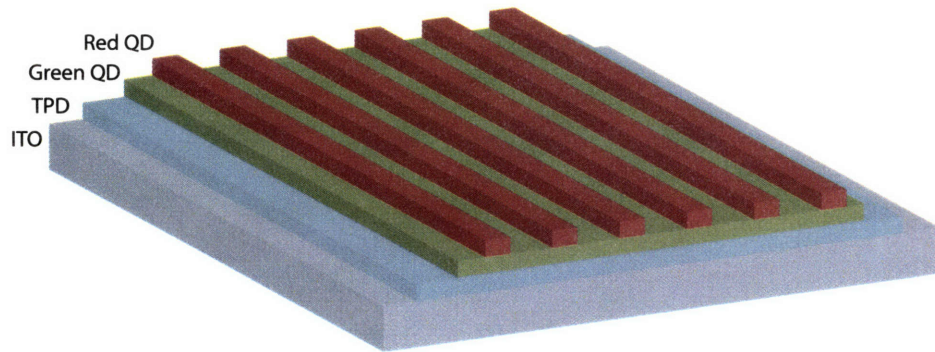
Figure 6-15: First three bottom layers in the device being operated in Fig. 6-16 and Fig. 6-18.

Figure 6-16: Lines of red quantum dots printed atop a full-plane green quantum dot film. An area where the PDMS did not contact the substrate when printing the green QDs shows the red QD emission as well as the organic. However, in all other areas, the luminescence of the red dots is much reduced.
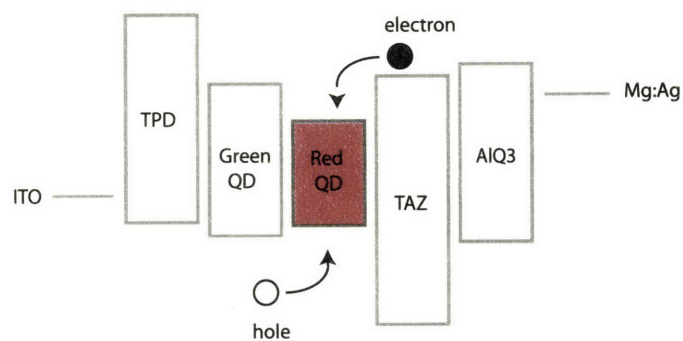
Figure 6-17: Cartoon showing that it would seem relaxation and luminescence is energetically favored to occur on the red QD film. Instead green emission is favored.
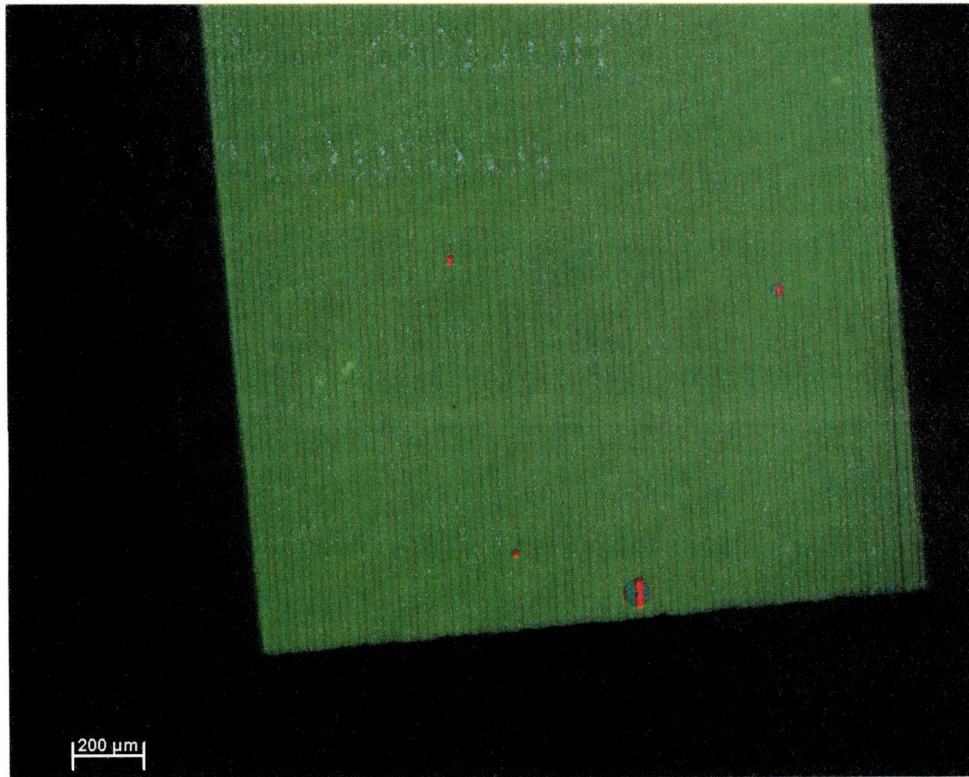
Figure 6-18: The same device as Fig. 6-16 except the green QD coverage is complete. The corresponding spectrum of this device is shown in Fig. 6-19 showing indeed there is very little red emission.
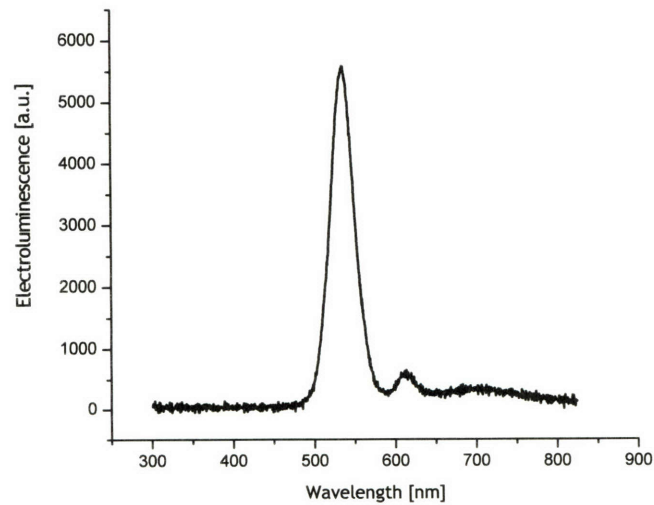
Figure 6-19: Spectrum of the device shown in Fig. 6-18, which shows minimal red QD emission and strong green QD emission.

Chapter 7

Conclusion

This work has demonstrated the capability to pattern quantum dots and to deposit the quantum dot film without exposing the underlying organic layer to solvents. We have shown red, green and blue devices with 1.2%, 0.5% and 0.25% quantum efficiencies, numbers similar to those of the phase separated devices. The CIE coordinates almost include the entire NTSC triangle. And the resolution is at least as good as 20 μm wide lines. Our demonstration of microcontact printing quantum dots has enabled the potential for QD-LED displays.

Much more work is needed before this method is a consistent, well-controlled one. Many important parameters, such as stamp thickness, applied pressures, curing steps, and parylene coating thickness were not carefully controlled. The large variability in those conditions produced a noticeable variability in the quality of quantum dot films. The next step is to methodically measure and correlate those variables to the printed films, and to better understand the mechanisms involved. However, we found it encouraging to observe the robustness of this process, despite the lack of attention paid to some of those parameters.

This work also provides the deposition of colloidal quantum dots a flexibility that has previously been missing. It will perhaps become a useful tool in probing the kinetics of quantum dots by providing good control over how and where they are placed in experimental setups, without the process being time-consuming. How dots interact when placed on top of each other, or within new kinds of device architectures

will be an interesting exploration to follow. Perhaps it will also aid others who are attempting other applications of quantum dots.

Bibliography

[1] Roger A. Freedman and William J. Kaufmann. *Universe*. New York : W.H. Freeman, 2005.

[2] Robert L. Myers. *Display Interfaces*. Chichester : Wiley, 2002.

[3] Lawrence E. Tannas, editor. *Flat-Panel Displays and CRTs*. New York : Van Nostran Reinhold Company, 1985.

[4] S.M. Kelly. *Flat Panel Displays, Advanced Organic Materials*. Royal Society of Chemistry, 2000.

[5] C.B. Murray, M. Nirmal, D.J. Norris, and M.G. Bawendi. Synthesis and structural characterization of II-VI semiconductor nanocrystallites (quantum dots). *Zeitschrift fur Physik D (Atoms, Molecules and Clusters)*, 26:231 – 3, 1993//.

[6] Younan Xia and George M. Whitesides. Soft lithography. *Annual Review of Materials Science*, 28:153 – 184, 1998.

[7] Dean J. Campbell, Katie J. Beckman, Camilo E. Calderon, Patrick W. Doolan, Rebecca M. Ottosen, Arthur B. Ellis, and George C. Lisensky. Replication and Compression of Bulk and Surface Structures with Polydimethylsiloxane Elastomer. *Journal of Chemical Education*, 76:537 – 541, 1999.

[8] Gautam Parthasarathy, Jie Liu, and Anil R. Duggal. Organic light emitting devices from displays to lighting. *Electrochemical Society Interface*, 12:42 – 47, 2003.

[9] Stephen R. Forrest. Active optoelectronics using thin-film organic semiconductors. *IEEE Journal on Selected Topics in Quantum Electronics*, 6:1072 – 1083, 2000.

[10] M. Pope, H.P. Kallmann, and P. Magnante. Electroluminescence in organic crystal. *Journal of Chemical Physics*, 38:2042 – 2043, 1963/04/15.

[11] W. Helfrich and W.G. Schneider. Recombination radiation in anthracene crystals. *Physical Review Letters*, 14:229 – 231, 1965/02/15.

[12] C.W. Tang and S.A. VanSlyke. Organic electroluminescent diodes. *Applied Physics Letters*, 51:913 – 15, 21 Sept. 1987.

[13] C.W. Tang, S.A. VanSlyke, and C.H. Chen. Electroluminescence of doped organic thin films. *Journal of Applied Physics*, 65:3610 – 16, 1989/05/01.

[14] J.H. Burroughes, D.D.C. Bradley, A.R. Brown, R.N. Marks, K. Mackay, R.H. Friend, P.L. Burns, and A.B. Holmes. Light-emitting diodes based on conjugated polymers. *Nature*, 347:539 – 541, 1990.

[15] A.P. Alivisatos. Semiconductor clusters, nanocrystals, and quantum dots. *Science*, 271:933 – 7, 1996/02/16.

[16] M. Nirmal and L. Brus. Luminescence photophysics in semiconductor nanocrystals. *ACCOUNTS OF CHEMICAL RESEARCH*, 32:407–414, 1999.

[17] Xiaogang Peng, Michael C. Schlamp, Andreas V. Kadavanich, and A.P. Alivisatos. Epitaxial growth of highly luminescent CdSe/CdS core/shell nanocrystals with photostability and electronic accessibility. *Journal of the American Chemical Society*, 119:7019 – 7029, 1997.

[18] V.L. Colvin, M.C. Schlamp, and A.P. Allvisatos. Light-emitting diodes made from cadmium selenide nanocrystals and a semiconducting polymer. *Nature*, 370:354 – 7, 1994/08/04.

[19] Seth Coe, Wing-Keung Woo, Moungi Bawendi, and Vladimir Bulovic. Electroluminescence from single monolayers of nanocrystals in molecular organic devices. *Nature*, 420:800 – 803, 2002.

[20] Seth Coe-Sullivan, Wing-Keung Woo, Jonathan S. Steckel, Moungi Bawendi, and Vladimir Bulovic. Tuning the performance of hybrid organic/inorganic quantum dot light-emitting devices. *Organic Electronics: physics, materials, applications*, 4:123 – 130, 2003.

[21] M.C. Schlamp, X. Peng, and A.P. Alivisatos. Improved efficiencies in light emitting diodes made with CdSe(CdS) core/shell type nanocrystals and a semiconducting polymer. *Journal of Applied Physics*, 82:5837 – 42, 1997/12/01.

[22] B. Michel, A. Bernard, A. Bietsch, E. Delamarche, M. Geissler, D. Juncker, H. Kind, J.-P. Renault, H. Rothuizen, H. Schmid, P. Schmidt-Winkel, R. Stutz, and H. Wolf. Printing meets lithography: soft approaches to high-resolution printing. *IBM Journal of Research and Development*, 45:697 – 719, Sept. 2001.

[23] Linda C. Hults. *The print in the western world : an introductory history.* University of Wisconsin Press, 1996.

[24] Y. N. Xia and G. M. Whitesides. Soft lithography. *ANGEWANDTE CHEMIE-INTERNATIONAL EDITION*, 37:551–575, 1998.

[25] A. Kumer and G.M. Whitesides. Features of gold having micrometer to centimeter dimensions can be formed through a combination of stamping with elastomeric stamp and an alkanethiol "ink" followed by chemical etching. *Applied Physics Letters*, 63:2002 – 4, 1993/10/04.

[26] Y. Xia. Soft lithography and the art of patterningA tribute to Professor George M. Whitesides. *ADVANCED MATERIALS*, 16:1245–1246, 2004.

[27] M.E. Schrader. Young. Dupre revisited. *Langmuir*, 11:3585 –, 1995.

[28] Kurt W. Kolasinski. *Surface science : foundations of catalysis and nanoscience.* Chichester ; New York : Wiley, 2002.

[29] University of Bolton Online Postgraduate Courses for the Electronics Industry. http://www.ami.ac.uk/courses/topics/0205_els/top.

[30] Dow Corning Website. http://www.dowcorning.com/content/sitech/sitechis/ what_makes_silicones_special.asp.

[31] M.K. Chaudhury. Interfacial interaction between low-energy surfaces. *Materials Science & Engineering R: Reports*, 16:97 – 159, 1996/03/.